



**HAL**  
open science

# Optimization of adiabatic control strategies along non-mixing curves with singularities

Nicolas Augier

► **To cite this version:**

Nicolas Augier. Optimization of adiabatic control strategies along non-mixing curves with singularities. 2021. hal-03270233

**HAL Id: hal-03270233**

**<https://inria.hal.science/hal-03270233>**

Preprint submitted on 24 Jun 2021

**HAL** is a multi-disciplinary open access archive for the deposit and dissemination of scientific research documents, whether they are published or not. The documents may come from teaching and research institutions in France or abroad, or from public or private research centers.

L'archive ouverte pluridisciplinaire **HAL**, est destinée au dépôt et à la diffusion de documents scientifiques de niveau recherche, publiés ou non, émanant des établissements d'enseignement et de recherche français ou étrangers, des laboratoires publics ou privés.

# Optimization of adiabatic control strategies along non-mixing curves with singularities

Nicolas Augier\*

June 24, 2021

## Abstract

In this paper, we consider a system driven by a controlled Schrödinger equation with two external control inputs. Motivated by applications to the control of quantum systems having conical or semi-conical eigenvalue intersections, we propose to study the singularities and the parametric bifurcations of the associated non-mixing field, along whose integral curves in the space of controls the adiabatic approximation holds with higher precision. Our results can be applied to optimize the adiabatic control strategies of well known quantum systems such as Qubit systems, Stirap Processes and Eberly-Law models.

**Keywords:** quantum control, adiabatic approximation, singularities

## 1 Introduction

Developing new mathematical tools enabling to optimize quantum adiabatic control strategies has attracted engineers and physicists in the last decades ([11, 17, 23, 25, 28]). Indeed, adiabatic methods, which provide regular and very robust control laws with respect to uncertainties and variations of the parameters (see for instance [4, 5, 9, 16, 24]) as a counterpart often require a long time of implementation. As a consequence, they seem to be difficult to implement experimentally, for instance in the case where physical states have short lifetimes.

In order to speed up quantum transitions, different methods have been introduced by physicists, such as shortcuts to adiabaticity [23, 27], and without resorting to adiabatic dynamics, one can mention the now commonly used quantum optimal control methods (see for instance [13] for a general review about such strategies). More generally, it appeared that a very precise mathematical study of the structure of quantum Hamiltonians can lead to improve the control methods used by experimentalists in a significant way.

In this context, we propose here to focus on a method which has been introduced in [8] and extended in [10] consisting in following particular adiabatic curves in the space of controls, called *non-mixing curves*. It turns out that those curves improve the precision of the adiabatic approximation and are directly linked to the geometry of the eigenstates of quantum Hamiltonians. The latter has already been shown to be linked to the controllability properties of the associated Schrödinger Equation [4, 5, 8], especially when considering Hamiltonians possessing eigenvalue intersections. As a byproduct, a crucial task is to understand the geometry of the non-mixing curves around eigenvalue intersections of the Hamiltonian, which play a major role in inducing adiabatic transitions of states.

In this paper, we propose to focus on the behavior of the non-mixing curves in the case of real Hamiltonians  $H(u, v)$  on a Hilbert space depending on two real control fields  $(u, v) \in \mathbb{R}^2$  around the

---

\*Inria, Université Côte d'Azur, INRAE, CNRS, Sorbonne Université, Biocore team, Sophia Antipolis, France

two least degenerate models of eigenvalue intersections (see [5]), namely the *conical intersection* (see Figure 1) and *semi-conical intersection* (see Figure 2).

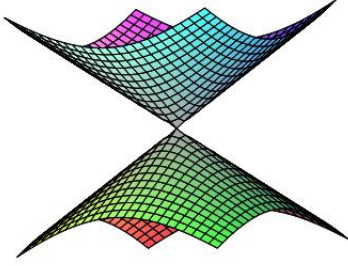


Figure 1: Conical intersection as a function of the controls  $(u, v) \in \mathbb{R}^2$ .

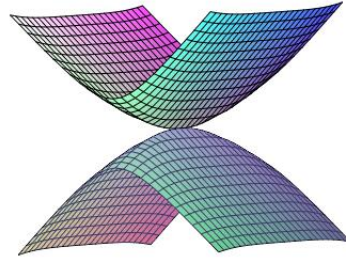


Figure 2: Semi-conical intersection of eigenvalues as a function of the controls  $(u, v) \in \mathbb{R}^2$ .

To this purpose, we consider a Hamiltonian  $H(u, v)$  on a Hilbert space  $\mathcal{H}$  and depending on two control parameters  $(u, v) \in \mathbb{R}^2$ , and the associated Schrödinger Equation

$$i \frac{d\psi(t)}{dt} = H(u(t), v(t))\psi(t), \quad (1)$$

where  $\psi(0) = \psi_0 \in \mathcal{H}$ ,  $\psi(t) \in \mathcal{H}$ , and  $(u(t), v(t)) \in \mathbb{R}^2$ .

An eigenvalue intersection  $(u, v) \in \mathbb{R}^2$  between two eigenvalues  $\lambda_{j-1}$  and  $\lambda_j$  of  $H$  is said to be

- *conical* if there exists  $C > 0$  such that

$$\frac{1}{C}t \leq |\lambda_j((u, v) + t\eta) - \lambda_{j-1}((u, v) + t\eta)| \leq Ct \quad (2)$$

for every unitary direction  $\eta \in \mathbb{R}^2 \setminus \{0\}$ , and  $t$  in a neighborhood of 0.

- *semi-conical* if there exists a unique unitary direction  $\eta \in \mathbb{R}^2 \setminus \{0\}$  up to multiplication by  $-1$ , called the *non-conical direction* at  $(u, v)$ , such that, for every smooth curve  $(\gamma(t))_{t \in [0,1]}$  of  $\mathbb{R}^2$  satisfying  $\gamma'(0) = \eta$ , we have

$$\frac{1}{C}t^2 \leq |\lambda_j((u, v) + \gamma(t)) - \lambda_{j-1}((u, v) + \gamma(t))| \leq Ct^2 \quad (3)$$

for some  $C > 0$  and  $t$  in a neighborhood of 0, and for every other direction  $\mu \in \mathbb{R}^2 \setminus \{0\}$  transversal to  $\eta$ , we have

$$\frac{1}{C}t \leq |\lambda_j((u, v) + t\mu) - \lambda_{j-1}((u, v) + t\mu)| \leq Ct \quad (4)$$

for some  $C > 0$  and  $t$  in a neighborhood of 0.

On the one hand, conical intersections are now well understood and are known to appear generically for real Hamiltonians which are driven by two real controls. Moreover they have been used

successfully to induce transitions of quantum states, both in the experimental and theoretical literature [4, 8, 10].

On the other hand, semi-conical intersections have been introduced in [5], in which the authors, motivated by the design of adiabatic control strategies which are robust with respect to an uncertain parameter, noticed that such singularities appear generically for one parameter families of Hamiltonians. They correspond to the case where the eigenvalues of the controlled Hamiltonian are transverse in every direction at the singularity excepted in a given direction  $\eta$  where they are tangent. The study of such eigenvalue intersections is very pertinent because they can be seen as a limit model of strongly inhomogeneous conical intersections, and this phenomenon appears in very classical models such as STIRAP processes or Eberly-Law system [1, 6] having two very close successive energy levels.

For a general Hamiltonian  $H$  depending on two real controls, the non-mixing curves between two discrete eigenvalues  $\lambda_{j-1}$  and  $\lambda_j$  for  $j \geq 2$  have been defined in [8] as the curves  $\gamma = (\gamma(\tau))_{t \in [0,1]}$  of  $\mathbb{R}^2$  along which the eigenvectors  $\phi_{j-1}$  and  $\phi_j$  associated with  $\lambda_{j-1}$  and  $\lambda_j$  are such that  $\dot{\phi}_{j-1}(\gamma(\tau))$  is orthogonal to  $\phi_j(\gamma(\tau))$  for the scalar product of  $\mathcal{H}$ , for every  $\tau \in [0, 1]$ . Qualitatively speaking, one can show that the error made in the adiabatic regime along a non-mixing curve does not depend on the gap between  $\lambda_{j-1}$  and  $\lambda_j$  nor on the variations of their associated eigenvectors but only on the gap between  $\{\lambda_{j-1}(\cdot), \lambda_j(\cdot)\}$  and the rest of the spectrum of  $H(\cdot)$  nor on the variations of the eigenvectors associated with  $\text{Spectrum}(H(\cdot)) \setminus \{\lambda_{j-1}(\cdot), \lambda_j(\cdot)\}$ . In particular, the error of order  $O(\sqrt{\epsilon})$  for a control path ending at a conical intersection between  $\lambda_{j-1}$  and  $\lambda_j$  (see [8]) is transformed into  $O(\epsilon)$  along a control path which follows a non-mixing curve.

The main goal of the paper is to continue the study started in [8] concerning the geometry of these curves, providing a classification of the singularities and normal forms at both conical and semi-conical eigenvalue intersections, and to deduce efficient methods to optimize quantum transition of states in both cases. Even if our study is mainly focused on the behavior around eigenvalue intersections, it is not limited to this case. Indeed, our study also tackles the case of Hamiltonians possessing very close eigenvalues, for which one of the experimental aims may be to guarantee the adiabaticity, that is, to avoid undesirable transitions between the corresponding quantum states.

The paper is organized as follows. In Section 2 we start by giving some basic definitions and results for the non-mixing field, which are essentially taken from [8]. Then in Sections 3 and 4, we focus on the case of two-level systems, and we classify the singularities of the non-mixing curves and their one-parameter bifurcations in this case, providing exact transitions between the eigenstates of the Hamiltonian. This leads us to define a new model of avoided-crossing, to the best of the author knowledge. In Section 5 we continue the analysis of the singularities of the non-mixing field started in [8] for general quantum systems and we prove that it has interesting topological properties. In particular it can exhibit both singularities having a half-integer index, which are usually generic for line fields on  $\mathbb{R}^2$ , and singularities having an integer index, usually generic for  $C^\infty$  vector fields on  $\mathbb{R}^2$ .

## 2 General definition of the non-mixing field

### 2.1 Definition of the non-mixing field, and known facts

#### 2.1.1 Adiabatic dynamics

Let  $\mathcal{H}$  be a separable Hilbert space, and  $\mathcal{L}_{sa}(\mathcal{H})$  be the set of essentially self-adjoint operators on  $\mathcal{H}$ . Denote the scalar product on  $\mathcal{H}$  by  $\langle \cdot, \cdot \rangle$ . Let  $V$  be a connected open set of  $\mathbb{R}^2$  and  $\gamma : [0, 1] \rightarrow V$  be a regular smooth control path. Let  $H(\cdot)$  be a bounded  $C^\infty$  function from  $V$  to  $\mathcal{L}_{sa}(\mathcal{H})$ , such that the operators  $H(u)$  have a common dense domain  $D \subset \mathcal{H}$  for every  $u \in V$ , and are bounded from below, uniformly with respect to  $u \in V$ . For every  $u \in V$ , denote the spectrum of  $H(u)$  by  $\sigma(u)$ .

**Assume in the following** that the two following conditions are satisfied.

**Assumption (GAP).** For a given  $j \geq 1$ ,  $\sigma_*(u) = \{\lambda_{j-1}(u), \lambda_j(u)\} \subset \sigma(u)$  is a locally discrete separated part of  $\sigma$ , for  $u \in V$ .

**Assumption (A).** The control path  $\gamma = (\gamma(\tau))_{\tau \in [0,1]}$  is a smooth regular curve of  $\mathbb{R}^2$  along which the eigenpairs  $(\lambda_k \circ \gamma, \phi_k \circ \gamma)_{k \in \{j-1, j\}}$  are  $C^\infty$ .

Let  $P_{j-1, j}(u)$  be the spectral projection of  $H(u)$  onto the eigenspace associated with  $\sigma_*(u)$ . For every  $\tau \in [0, 1]$ , consider a unitary mapping  $\mathcal{U}(\tau)$  from  $\mathbb{C}^2$  to  $\text{Im}P_{j-1, j}(\gamma(\tau))$ , which is  $C^\infty$  with respect to  $\tau \in [0, 1]$ , such that  $\mathcal{U}(\tau)(e_1) = \phi_{j-1}(\gamma(\tau))$  and  $\mathcal{U}(\tau)(e_2) = \phi_j(\gamma(\tau))$ , where  $(e_1, e_2)$  is the canonical basis of  $\mathbb{C}^2$ . Then the Effective Hamiltonian associated with  $H$  and the transformation  $\mathcal{U}$  reads

$$H_{\text{eff}}(\gamma(\tau)) = \begin{pmatrix} \lambda_{j-1}(\gamma(\tau)) & 0 \\ 0 & \lambda_j(\gamma(\tau)) \end{pmatrix} - i\epsilon \begin{pmatrix} 0 & \langle \dot{\phi}_{j-1}(\gamma(\tau)), \phi_j(\gamma(\tau)) \rangle \\ \langle \dot{\phi}_j(\gamma(\tau)), \phi_{j-1}(\gamma(\tau)) \rangle & 0 \end{pmatrix}, \quad (5)$$

where  $\dot{\phi}_q(\gamma(\tau))$ ,  $q \in \{j-1, j\}$  is the derivative of  $\phi_q$  along the path  $\gamma$ . Denoting the propagator of equation

$$i\epsilon \frac{d\psi(\tau)}{d\tau} = H(\gamma(\tau))\psi(\tau) \quad (6)$$

by  $U^\epsilon(\tau)$  and the propagator of Equation

$$i\epsilon \frac{d\psi(\tau)}{d\tau} = H_{\text{eff}}(\gamma(\tau))\psi(\tau)$$

by  $U_{\text{eff}}^\epsilon(\tau)$ , the adiabatic approximation theorem (see, [26, Theorem 1.4]) yields

$$\| (U^\epsilon(\tau) - \mathcal{U}(\gamma(\tau))U_{\text{eff}}^\epsilon(\tau)\mathcal{U}^{-1}(\gamma(0))) P_{j-1, j}(0) \| \leq C\epsilon, \quad (7)$$

for every  $\tau \in [0, 1]$ , where  $C > 0$  is independent of  $\epsilon > 0$ .

### 2.1.2 Definition of the non-mixing curves

**Definition 2.1.** For a general Hamiltonian  $H$  depending on two real controls, the non-mixing curves between  $\lambda_{j-1}$  and  $\lambda_j$  for  $j \geq 2$  have been defined in [8] as the curves  $\gamma = (\gamma(\tau))_{\tau \in [0,1]}$  of  $\mathbb{R}^2$  along which  $\dot{\phi}_{j-1}(\gamma(\tau))$  is orthogonal to  $\phi_j(\gamma(\tau))$ , for every  $\tau \in [0, 1]$ .

**Remark 2.2.** Notice that the previous definition does not depend on the smooth regular parametrization of  $\gamma$ , in the sense that if  $(c(\tau))_{\tau \in [0,1]}$  is a smooth regular parametrization of a non-mixing curve  $\gamma$  and  $\varphi$  is a regular time reparametrization of  $[0, 1]$ , then  $((c \circ \varphi)(\tau))_{\tau \in [0,1]}$  is such that  $\dot{\phi}_{j-1}((c \circ \varphi)(\tau))$  is orthogonal to  $\phi_j((c \circ \varphi)(\tau))$  for every  $\tau \in [0, 1]$ .

As a direct consequence of Equation (7), we get the following result.

**Proposition 2.3.** Assume that Assumption (A) holds. Let  $\psi_0 = \phi_j(\gamma(0))$  and for every  $\tau \in [0, 1]$ ,  $\psi_\epsilon(\tau) = U^\epsilon(\tau)\psi_0$ . If  $\gamma$  is a non-mixing curve, then we have, for every  $\epsilon > 0$ ,  $\|\psi_\epsilon(\tau) - e^{i\eta}\phi_j(\gamma(\tau))\| \leq C\epsilon$ , for  $\tau \in [0, 1]$ , where  $\eta$  is possibly depending on  $\epsilon$ , and  $C > 0$  is independent of  $\epsilon$ .

The constant  $C > 0$  only depends on  $[0, 1] \ni \tau \mapsto \text{Dist}(\sigma^*(\gamma(\tau)), \sigma(\gamma(\tau)) \setminus \sigma^*(\gamma(\tau)))$  and related quantities (see, for instance [26, Theorem 2.2.]), and, in particular, it does not depend directly on the gap  $[0, 1] \ni \tau \mapsto \lambda_j(\gamma(\tau)) - \lambda_{j-1}(\gamma(\tau))$ . In particular, Proposition 2.3 allows to follow non-mixing curves passing at intersections of eigenvalues while guaranteeing that the adiabatic error is not deteriorated at the singularity, independently of the geometry of the eigenvalues. This fact motivates the analysis of the behavior of the non-mixing curves around intersections of eigenvalues.

In order to enable such a study, we present the following result can be deduced from [8, Section V].

**Proposition 2.4.** *The non-mixing curves between two eigenvalues  $\lambda_{j-1}(\cdot)$  and  $\lambda_j(\cdot)$  of  $H(\cdot)$  are the integral curves of a line field on  $\mathbb{R}^2$ , called non-mixing field, which is defined up to a sign, for  $(u, v) \in V$ , by  $\chi_{j-1,j}(u, v) = \begin{pmatrix} -\langle \partial_2 H(u, v) \phi_{j-1}(u, v), \phi_j(u, v) \rangle \\ \langle \partial_1 H(u, v) \phi_{j-1}(u, v), \phi_j(u, v) \rangle \end{pmatrix}$ .*

## 2.2 Singularities of the non-mixing curves at conical intersections and application in control

In this section, we recall some known results from [8] concerning the singularities of the non-mixing curves at conical intersections of eigenvalues in the case of real Hamiltonians which are affine in the controls  $(u, v) \in V$ .

**Assumption ( $\mathcal{R}$ ).** *For every  $(u, v) \in V$ ,  $H(u, v) = H_0 + uH_1 + vH_2$  where  $H_0, H_1, H_2$  are essentially self-adjoint operators on  $\mathcal{H}$  having a common dense domain  $\mathcal{D} \subset \mathcal{H}$  such that:*

- $H_0$  has a discrete spectrum;
- $H_1, H_2$  are bounded;
- There exists an orthonormal basis  $(b_j)_j$  of the Hilbert space  $\mathcal{H}$  such that  $\langle b_j, H_0 b_q \rangle, \langle b_j, H_1 b_q \rangle, \langle b_j, H_2 b_q \rangle$  are real for every  $j, q$ .

Note that the third condition means qualitatively that we can find of basis of  $\mathcal{H}$  in which the Hamiltonian  $H(u, v)$  is real.

**Singularities of the non-mixing curves at conical intersections.** When Assumption ( $\mathcal{R}$ ) holds true, in a neighborhood of a conical intersection  $(\bar{u}, \bar{v}) \in \mathbb{R}^2$  between the levels  $j - 1$  and  $j$ ,

- For every  $(u, v) \neq (\bar{u}, \bar{v})$ , there exists a smooth choice of the sign of the eigenvectors  $\phi_{j-1}(u, v)$  and  $\phi_j(u, v)$  such that  $\chi_{j-1,j}$  defines a  $C^\infty$  vector field in a punctured neighborhood of  $(\bar{u}, \bar{v})$ ,
- The integral curves of  $\chi_{j-1,j}$  are  $C^\infty$  and the eigenvectors  $\phi_{j-1}$  and  $\phi_j$  are  $C^\infty$  along them,
- For every direction  $\eta$  of  $\mathbb{R}^2$ , there exists an integral curve  $\gamma : [0, 1) \rightarrow \mathbb{R}^2$  of  $\chi_{j-1,j}$  such that  $\lim_{t \rightarrow 1^-} \gamma(t) = (\bar{u}, \bar{v})$ ,  $\lim_{t \rightarrow 1^-} \frac{\dot{\gamma}(t)}{\|\dot{\gamma}(t)\|} = \eta$ .

We say that the singularity of  $\chi_{j-1,j}$  has type **(N)**, for node. In particular the third condition implies that the non-mixing curves are homeomorphic to the integral curves of the vector field  $(u, v) \mapsto \begin{pmatrix} u - \bar{u} \\ v - \bar{v} \end{pmatrix}$  locally around  $(\bar{u}, \bar{v})$  and the index of  $\chi_{j-1,j}$  at  $(\bar{u}, \bar{v})$  is equal to 1.

**Application in control.** By using concatenations of two non-mixing curves having different directions at the singularity, it was proved in [8, Proposition 6.1.] that it is possible to build, for any arbitrary  $(p_{j-1}, p_j) \in \mathbb{S}^1$ , a piecewise  $C^\infty$  control path  $(\gamma(\tau))_{\tau \in [0, 1]}$ , such that  $\psi_\epsilon(0) = \phi_{j-1}(\gamma(0))$ , and for every  $\epsilon > 0$ ,

$$\|\psi_\epsilon(1/\epsilon) - p_{j-1} e^{\beta_{j-1}} \phi_{j-1}(\gamma(1)) - p_j e^{\beta_j} \phi_j(\gamma(1))\| \leq C\epsilon,$$

where  $C > 0$  is independent of  $\epsilon$ , and  $\beta_{j-1}, \beta_j \in \mathbb{R}$ .

### 3 The non-mixing field for two level systems: singularities and parametric bifurcations

In this section, we focus on some features of the non-mixing curves which are specific to two-level systems. In this case, the non-mixing curves can be identified as the integral curves of a smooth vector field, called *regular non-mixing field* defined in Proposition 3.3 on  $\mathbb{R}^2$ , which vanishes at the eigenvalue intersections, and the adiabatic error is equal to zero along them. Note that, for control purposes, the aim will be to reach the intersections of eigenvalues in finite time. In general, this will not be guaranteed by following the integral curves of the regular non-mixing field, contrarily to what happens with the non-mixing field defined as in Definition 2.4. However, once a control path  $(\gamma(t))_{t \in [0,1]}$  is chosen, every smooth reparametrization of this path provides the same non-mixing property in the adiabatic regime (see Remark 2.2).

#### 3.1 Particular features

Let  $f = (f_1, f_2) \in C^\infty(\mathbb{R}^2, \mathbb{R}^2)$  and define the Hamiltonian  $H_f(u, v) = \begin{pmatrix} f_1(u, v) & f_2(u, v) \\ f_2(u, v) & -f_1(u, v) \end{pmatrix}$ . Consider a smooth regular control path  $\gamma(t) = (u(t), v(t))_{t \in [0,1]}$  such that there exist  $P \in C^2([0, 1], \text{SO}_2(\mathbb{R}))$  and  $\lambda \in C^k([0, 1], \mathbb{R})$  for  $k \in \mathbb{N}$  such that  $\{\lambda(t), -\lambda(t)\}$  is the spectrum of  $H_f(u, v)$  and the columns of  $P$  form a basis of eigenvectors of  $H_f(\gamma(t))$  for every  $t \in [0, 1]$ . We can write, for every  $t \in [0, 1]$ ,  $P(t) = \begin{pmatrix} \cos(\theta(t)) & -\sin(\theta(t)) \\ \sin(\theta(t)) & \cos(\theta(t)) \end{pmatrix}$  where  $\theta \in C^2([0, 1], \mathbb{R})$ .

Let us study the dynamics of

$$i \frac{d\psi_\epsilon(t)}{dt} = H_f(u(t), v(t))\psi(t), \quad \psi(0) = \tilde{\psi}_0, \quad (8)$$

where  $t \in [0, 1]$  and  $\tilde{\psi}_0 \in \mathbb{C}^2$ .

Defining  $Y(t) = P(t)\psi(t)$  for every  $t \in [0, 1]$ , we have

$$i \frac{dY(t)}{dt} = \left( \begin{pmatrix} \lambda(t) & 0 \\ 0 & -\lambda(t) \end{pmatrix} + \begin{pmatrix} 0 & i\dot{\theta}(t) \\ -i\dot{\theta}(t) & 0 \end{pmatrix} \right) Y(t). \quad (9)$$

Using the previous notations, we have that  $\gamma$  is a non-mixing curve in the sense of Definition 2.1 if it satisfies  $\dot{\theta}(t) = 0$ , for every  $t \in [0, 1]$ . Hence it follows that, along a non-mixing curve  $\gamma$ , the error occurring in the adiabatic approximation is equal to 0, that is, the non-mixing curves can be followed at an arbitrary speed.

**Lemma 3.1.** *Let  $(\gamma(t))_{t \in [0,1]}$  be a non-mixing curve. Then, the solution  $\psi(t)$  of Equation (8) such that  $\psi_0 = \phi_j(\gamma(0))$  satisfies  $\psi(t) = e^{i\eta} \phi_j(\gamma(t))$ , for  $t \in [0, 1]$ , where  $\eta \in \mathbb{R}$ .*

By a direct computation of the eigenvectors of  $H_f$ , we show the following

**Proposition 3.2.**  *$\gamma$  is a non-mixing curve of  $H_f$  if and only if there exists  $(c_1, c_2) \in \mathbb{R}^2 \setminus \{(0, 0)\}$  such that*

$$c_1 f_1(\gamma(t)) + c_2 f_2(\gamma(t)) = 0, \quad (*)$$

for every  $t \in [0, 1]$ .

Next proposition states that the non-mixing curves of a two-level system are the integral curves of a smooth vector field on  $\mathbb{R}^2$ .

**Proposition 3.3.** *The non-mixing curves of  $H_f$  are the non trivial integral curves of the  $C^\infty$  vector field  $\chi(f) = \begin{pmatrix} f_1\partial_2f_2 - f_2\partial_2f_1 \\ f_2\partial_1f_1 - f_1\partial_1f_2 \end{pmatrix}$ , called the regular non-mixing field.*

*Proof.* Let  $(\gamma(t))_{t \in [0,1]}$  be a regular smooth curve of  $\mathbb{R}^2$  and let  $t_0 \in [0, 1]$ . Assume that  $f_2(\gamma(t)) \neq 0$ , for every  $t$  in a neighborhood  $V$  of  $t_0$ . Then  $\gamma$  satisfies Equation (\*) for every  $t \in V$  if and only if  $\frac{f_1(\gamma(\cdot))}{f_2(\gamma(\cdot))}$  is constant on  $V$ . Provided that  $\frac{f_1}{f_2}$  is  $C^\infty$  in a neighborhood of  $\gamma(t_0)$ , we deduce that the previous condition is satisfied if and only if, for every  $t \in V$ ,  $\gamma'(t)$  is orthogonal to  $\nabla \frac{f_1}{f_2}(\gamma(t))$ . Hence,  $\gamma$  is an integral curve of  $\chi(f)$ , up to a time reparametrization. The same holds if  $f_1(\gamma(t)) \neq 0$ , for every  $t$  in a neighborhood of  $t_0$ .  $\square$

## 3.2 Non-mixing curves at conical and semi-conical singularities

In this section, we define two models for the non-mixing field for Hamiltonians corresponding to the normal forms taken from [5, Section 2.3.], that are recalled in Appendix A.2. Their related genericity properties will be discussed in Section 4, and here we restrict our study to the main specific features of those models.

The first model is the conical intersection, which corresponds to  $f_1(u, v) = u$  and  $f_2(u, v) = v$ , for every  $(u, v) \in \mathbb{R}^2$ . In this case, for every  $(u, v) \in \mathbb{R}^2$ ,  $\chi(f)(u, v) = \begin{pmatrix} u \\ v \end{pmatrix}$ , and the corresponding singularity is called a *critical node*.

**Definition 3.4.** *Define semi-conical singularities as the singularities of the non-mixing field of  $f = (f_1, f_2) \in C^\infty(\mathbb{R}^2, \mathbb{R}^2)$  such that  $f_1(u, v) = h(u)u$ ,  $f_2(u, v) = u + v^2$  for every  $(u, v) \in \mathbb{R}^2$ , where  $h \in C^\infty(\mathbb{R}, \mathbb{R})$  is a smooth function such that  $h(0) = 1$ .*

We introduce the following condition:

$$h'(0) \neq 0. \tag{L}$$

Assume in this section that Condition (L) holds. We are going to prove that the semi-conical singularities have two possible behaviors, depending on the sign of  $h'(0)$ .

In this case, the regular non-mixing field is defined (see Proposition 3.3) as

$$\chi(u, v) = \begin{pmatrix} 2vuh(u) \\ u^2h'(u) + v^2uh'(u) + v^2h(u) \end{pmatrix}.$$

From Proposition 3.2, for  $f \in C^\infty(\mathbb{R}^2, \mathbb{R}^2)$ ,  $\gamma$  is a non-mixing curve of  $H_f$  if and only if there exists  $(c_1, c_2) \in \mathbb{R}^2 \setminus \{(0, 0)\}$  such that

$$0 = c_1f_1(\gamma(t)) + c_2f_2(\gamma(t)) = c_1u(t)h(u(t)) + c_2(u(t) + v(t)^2), \tag{*}$$

for every  $t \in [0, 1]$ .

Defining  $\forall (u, v) \in U$ ,  $F_c(u, v) = uh(u) - cu - cv^2$ , the set of the non mixing curves is the union of the curves along which  $F_c$  is equal to zero for some  $c \in \mathbb{R}$  with the parabola of equation  $u + v^2 = 0$ .

**Proposition 3.5.** *For  $c \neq 1$ ,  $F_c(u, v) = 0 \iff u = \phi_c(v)$ , where  $\phi_c \in C^\infty(\mathbb{R}, \mathbb{R})$  satisfies  $\phi_c'(0) = 0$  and  $\phi_c''(0) = \frac{2c}{1-c}$ .*

*Proof.* Assume  $c \neq 1$ . By direct computations, we have  $\frac{\partial F_c}{\partial u} = h(u) + uh'(u) - c$ . Evaluating at  $u = 0$  and using the condition  $h(0) = 1$ , we get  $\frac{\partial F_c}{\partial u} \Big|_{(0,0)} = 1 - c \neq 0$ . The Implicit Function Theorem ensures the existence of  $\phi_c \in C^\infty(\mathbb{R}, \mathbb{R})$  satisfying  $\phi_c(0) = 0$  such that  $F_c(u, v) = 0 \iff u = \phi_c(v)$ , for every  $(u, v)$  in a neighborhood of  $(0, 0)$ . Differentiating twice the relation  $F_c(\phi_c(v), v) = 0$  w.r.t.  $v$ , we get  $\phi_c'(0) = 0$  and  $\phi_c''(0) = \frac{2c}{1-c}$ .  $\square$



**Theorem 3.6.** *The set  $\{(u, v) \in U \mid F_1(u, v) = 0\}$  is diffeomorphic to  $\{(0, 0)\}$  or  $\{(u, v) \in U, |u| = |v|\}$ .*

*Proof.* Consider the function  $g$  defined by  $g(u) = h(u) - 1$ . Under assumption **(L)**, we have  $g(0) = 0$  and  $g'(0) = h'(0) \neq 0$ . Then we get the equivalence

$$F_1(u, v) = 0 \iff v^2 = ug(u),$$

for every  $(u, v) \in \mathbb{R}^2$ . If  $g'(0) < 0$ , the previous equation has no solution but  $u = v = 0$ . If  $g'(0) > 0$ , we can write  $g(u) = u(g'(0) + u\tilde{g}(u))$ , where  $\tilde{g} \in C^\infty(\mathbb{R}, \mathbb{R})$  satisfies  $\tilde{g}(0) \neq 0$ . Then we have  $F_1(u, v) = 0 \iff v^2 = u^2\tilde{g}(u) = u^2(g'(0) + ug_1(u))$ . Applying the right diffeomorphic transformation  $(u, v) \mapsto \begin{pmatrix} u\sqrt{g'(0) + ug_1(u)} \\ v \end{pmatrix}$ , we have in new coordinates  $F_1(u, v) = 0 \iff v^2 = u^2$ . □

We have shown that the non-mixing curves can have two different behaviours depending on the sign of  $h'(0)$ :

- The case where  $h'(0) < 0$  that we refer as the *Elliptic semi-conical singularity* (see Figure 3). 0 is an index 2 singularity for the vector field  $\chi$ . Every non-mixing curve passes through 0 and is tangent to the non-conical direction at 0.
- The case where  $h'(0) > 0$  that we refer as the *Hyperbolic semi-conical singularity* (see Figure 4). 0 is an index zero singularity for the vector field  $\chi$ . Every non-mixing curve passing at the origin is tangent to the non-conical direction except the level  $c = 1$  which passes through the origin in a conical direction (see the red curves on Figure 4). There exist also some non-mixing curves which do not pass through the origin. Notice that even if the index of the singularity is equal to zero, the non-mixing curves are not homeomorphic to the integral curves of a non-singular vector field at 0.

We can achieve an homogeneous blow-up in the polar coordinates  $(r, \theta) \in \mathbb{R} \times \mathbb{S}^1$ . Then the origin is blown up to  $\mathbb{S}^1$ . In polar coordinates, the non-mixing field  $\chi$  is transformed into

$$\tilde{\chi}(r, \theta) = \eta_1(r, \theta) \frac{\partial}{\partial \theta} + \eta_2(r, \theta) r \frac{\partial}{\partial r},$$

where

$$\eta_1(r, \theta) = \cos^3(\theta)h'(r \cos(\theta)) - \cos(\theta) \sin^2(\theta)h(r \cos(\theta)) + r \cos^2(\theta) \sin^2(\theta)h'(r \cos(\theta)),$$

and

$$\begin{aligned} \eta_2(r, \theta) = & \cos(\theta) \sin(2\theta)h(r \cos(\theta)) + \sin(\theta) \cos^2(\theta)h(r \cos(\theta)) \\ & + \sin^3(\theta)h(r \cos(\theta)) + r \sin^3(\theta) \cos(\theta)h'(r \cos(\theta)). \end{aligned}$$

By direct computations, we prove that the singularities of  $\tilde{\chi}$  on  $\{0\} \times \mathbb{S}^1$  are hyperbolic. More precisely, we can show that an elliptic semi-conical singularity can be desingularized into two nodes (one attractive and one repulsive) for a value of the angle  $\theta = \pm \frac{\pi}{2}$  (see Figure 5). By classical results on hyperbolic singularities of vector fields (see [12]), we deduce that the non-mixing curves are in this case homeomorphic to those obtained with  $h(u) = 1 - u$  for every  $u$ . On the other hand, an hyperbolic semi-conical singularity can be desingularized into two nodes for a value of the angle  $\theta = \pm \frac{\pi}{2}$  and four saddles for the angles  $\theta$  such that  $(\tan(\theta))^2 = h'(0)$  (see Figure 6). We can deduce that the non-mixing curves are in this case homeomorphic to those obtained with  $h(u) = 1 + u$  for every  $u$ .

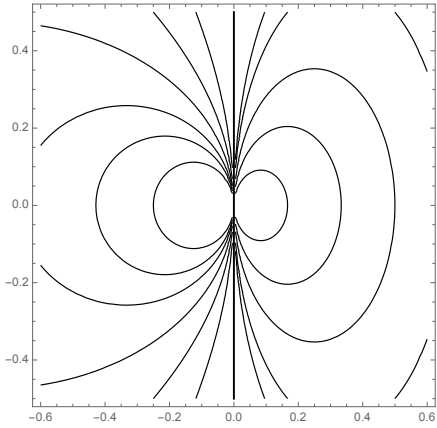


Figure 3: An example of *elliptic semi-conical singularity* with  $h(u) = 1 - u$  for every  $u$ . The non-conical direction is  $(0,1)$ . Every non-mixing curve passes through the singularity in the non-conical direction. The index is 2.

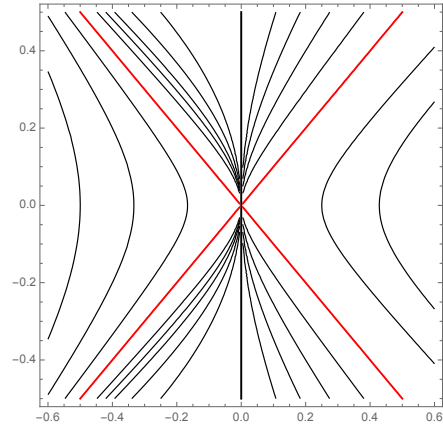


Figure 4: A example of *hyperbolic semi-conical singularity* with  $h(u) = 1 + u$  for every  $u$ . The non-conical direction is  $(0,1)$ . The red curves are the only non-mixing curves passing through the singularity in conical directions. The index is 0.

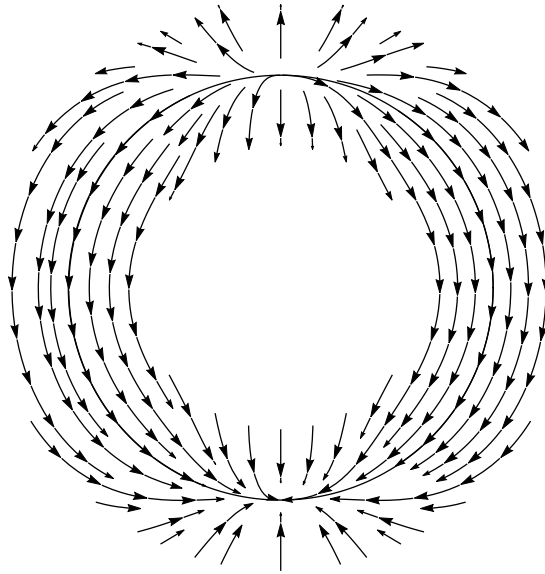


Figure 5: Elliptic semi-conical singularity in the coordinates  $(r, \theta) \in \mathbb{R} \times \mathbb{S}^1$  after desingularization with  $h(u) = 1 - u$  for every  $u$ .

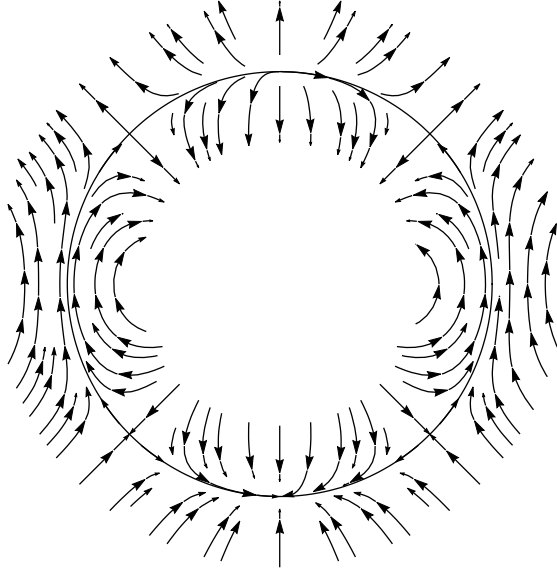


Figure 6: Hyperbolic semi-conical singularity in the coordinates  $(r, \theta) \in \mathbb{R} \times \mathbb{S}^1$  after desingularization with  $h(u) = 1 + u$  for every  $u$ .

### 3.3 Applications in control: achieving precise state superpositions at semi-conical intersections

In this section, we propose a method of optimization of adiabatic control strategies for two-level quantum systems having semi-conical intersections of eigenvalues, in analogy with the results stated in Section 2.2. In the case of semi-conical intersections, notice that for a path  $\gamma$  passing through the eigenvalue intersection in the non-conical direction, we obtain thanks to [5, Proposition 17] that the limit behavior of the eigenstates of the Hamiltonian at the singularity depends on the value of  $\tilde{\gamma}$ , as it will be stated in Proposition 3.7 (instead of  $\hat{\gamma}$  at conical intersections, see [8, Proposition 4.5]). As a result of this fact, we are going to see that in this case, one can induce superpositions of states for quantum systems with  $n \times n$  real Hamiltonians with  $n \geq 2$  possessing semi-conical intersections. This is made possible by considering piecewise  $C^2$  paths in the non-conical direction having a discontinuity on  $\tilde{\gamma}$  at the semi-conical eigenvalue intersection (qualitatively speaking, such a path has a second order angle at the singularity), instead of using piecewise  $C^1$  paths with angles at conical eigenvalue intersections. Then we will use the results of Section 3.2 to propose an improvement of such a control method specific to two-level systems, by considering control paths that follow some well chosen non-mixing curves.

#### 3.3.1 Superposition of states for $n \times n$ Hamiltonians with semi-conical intersections

In this section, we consider a real  $n \times n$  with  $n \geq 2$  Hamiltonian  $H(u, v)$  having a semi-conical intersection between the levels  $\lambda_{j-1}$  and  $\lambda_j$  at 0, for  $j \geq 2$ . Without loss of generality, we can assume that the non-conical direction is  $e_2$ . By the results of [5, Section 6], the limit behavior of the eigenstates of  $H(u, v)$  at the eigenvalue intersection can be deduced from the study of the normal form obtained for two-level systems having a semi-conical intersection. In this purpose, let

$f : (u, v) \mapsto \begin{pmatrix} h(u)u \\ u + v^2 \end{pmatrix}$  be the normal form of semi-conical intersections (see Appendix A.8),  $H_f$  its associated two-level Hamiltonian. Consider a smooth control path  $\gamma(t) = (u(t), v(t))_{t \in [0,1]}$  and  $t_0 \in (0, 1)$  such that  $\gamma(t_0) = (0, 0)$ ,  $\dot{u}(t_0) = 0$  and  $\dot{v}(t) = 1$ , for every  $t \in [0, 1]$ . A direct property concerning the limit eigenvector basis at the singularity is the following. It can be deduced directly from [5, Proposition 17].

**Proposition 3.7** ( $C^2$  angles in the non-conical direction). *Consider a piecewise  $C^2$  constant speed path  $\gamma$  such that  $\gamma(t_0) = (0, 0)$ , and set  $\ddot{u}(t_0^-) = a$ ,  $\ddot{u}(t_0^+) = a'$ . Then the basis  $(\phi_1, \phi_2)$  of eigenvectors of  $H_f$  is such that*

$$\begin{aligned} \lim_{t \rightarrow t_0^+} \phi_1(\gamma(t)) &= \cos(\theta(a) - \theta(a')) \lim_{t \rightarrow t_0^-} \phi_1(\gamma(t)) + \sin(\theta(a) - \theta(a')) \lim_{t \rightarrow t_0^-} \phi_2(\gamma(t)) \\ \lim_{t \rightarrow t_0^+} \phi_2(\gamma(t)) &= -\sin(\theta(a) - \theta(a')) \lim_{t \rightarrow t_0^-} \phi_1(\gamma(t)) + \cos(\theta(a) - \theta(a')) \lim_{t \rightarrow t_0^-} \phi_2(\gamma(t)), \end{aligned}$$

where for every  $x \in \mathbb{R}$ ,  $\theta(x) = \arctan(f(x))$  with  $f(x) = -\frac{2}{x} \left( 1 + \frac{x}{2} - \sqrt{1 + x + \frac{x^2}{2}} \right)$ .

We have plotted the function  $\theta$  on Figure 7.

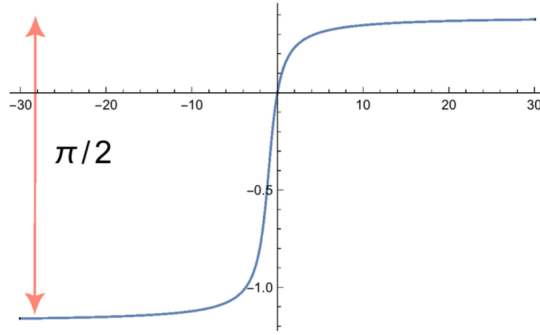


Figure 7: The function  $\theta$  as a function of  $x$ .

Proposition 3.7 on the semi-conical normal form allows to deduce the following existence result for general  $n$ -level systems having a semi-conical intersection at 0. However, by an extension of what was done in [8, Proposition 4.5], one could have specified the suitable second order angle needed to achieve a prescribed state superposition. Without loss of generality, one can assume that the non-conical direction is  $e_2$ .

**Proposition 3.8.** *Set  $n \geq 2$ , and let  $H(u, v)$  be a  $n \times n$  real Hamiltonian having a semi-conical intersection between the levels  $\lambda_{j-1}$  and  $\lambda_j$  at 0, for  $j \geq 2$ , in direction  $e_2$ . Let  $p_{j-1} \in (0, 1]$  and  $p_j \in [0, 1)$  be such that  $p_{j-1}^2 + p_j^2 = 1$ . Then there exist  $(a, a') \in \mathbb{R}$  and a piecewise  $C^2$  constant speed path  $\gamma(t) = (u(t), v(t))_{t \in [0,1]}$  where  $\gamma$  passes at the singularity in the non-conical direction  $e_2$  at time  $t = t_0 \in [0, 1]$  and  $\ddot{u}(t_0^-) = a$ ,  $\ddot{u}(t_0^+) = a'$ , such that the solution  $\psi_\epsilon(t) \in \mathbb{C}^n$  of Equation (6) with  $|\langle \psi_\epsilon(0), \phi_{j-1}(\gamma(0)) \rangle| = 1$  satisfies  $\|\psi_\epsilon(1/\epsilon) - p_{j-1}e^{i\eta_{j-1}}\phi_{j-1}(\gamma(1)) - p_je^{i\eta_j}\phi_j(\gamma(1))\| \leq C\epsilon^{1/3}$  where  $\eta_{j-1}, \eta_j \in \mathbb{R}$ , and  $C > 0$  independent of  $\epsilon > 0$ .*

**Remark 3.9.** *A complete transition from  $\phi_{j-1}$  to  $\phi_j$  (i.e.  $|\theta(a) - \theta(a')| = \frac{\pi}{2}$ ) is impossible by this method excepted if  $\ddot{u}(t_0^-) \rightarrow -\infty$  and  $\ddot{u}(t_0^+) \rightarrow +\infty$ . This case corresponds to the limit case when the path  $\gamma$  passes through the singularity in a conical direction (i.e. a direction which is transverse to the non-conical direction).*

### 3.3.2 Use of the non-mixing curves for two-level systems

In this section, we propose a control strategy which optimizes the adiabatic error given in Proposition 3.8 in the case of two-level systems. It consists in choosing a control path which follows successively two suitable non-mixing curves making a prescribed second order angle between them at the singularity. The key ingredient is that, in the case of two-level systems satisfying Condition **(L)**, Proposition 3.5 ensures that for every  $\alpha \in \mathbb{R}$ , there exists a non-mixing curve that can be parametrized as  $u = c_\alpha(v)$  with a smooth function  $c_\alpha$  such that  $c_\alpha(0) = c'_\alpha(0) = 0$  and  $c''_\alpha(0) = \alpha$ . As a by-product of the propositions 3.7 and 3.8, it follows that it is possible to induce exact superpositions of states by using control paths passing through the singularity in the non-conical direction with second order angles at the singularity. Such a control path can be followed at an arbitrary speed and follows the non-mixing curves of the Hamiltonian.

**Proposition 3.10.** *Let  $f \in C^\infty(\mathbb{R}^2, \mathbb{R}^2)$  be such that its associated Hamiltonian  $H_f$  has a semi-conical intersection in direction  $e_2$  at 0. Given  $p_1 \in (0, 1]$  and  $p_2 \in [0, 1)$  such that  $p_1^2 + p_2^2 = 1$ , consider a piecewise  $C^2$  constant speed path  $\gamma(t) = (u(t), v(t))_{t \in [0, 1]}$  such that  $\gamma$  passes at the singularity in the non-conical direction  $e_2$  at time  $t = t_0 \in [0, 1]$ . Then there exist  $(a, a') \in \mathbb{R}^2$  such that, if  $\ddot{u}(t_0^-) = a, \ddot{u}(t_0^+) = a'$ , then the solution  $\psi(t) \in \mathbb{C}^2$  of Equation (8) such that  $|\langle \psi(0), \phi_1(\gamma(0)) \rangle| = 1$  satisfies  $\psi(1) = p_1 e^{i\eta_1} \phi_1(\gamma(1)) + p_2 e^{i\eta_2} \phi_2(\gamma(1))$  where  $\eta_1, \eta_2 \in \mathbb{R}$ .*

Now consider  $p_1 \in (0, 1]$  and  $p_2 \in [0, 1)$  such that  $p_1^2 + p_2^2 = 1$ , and  $(a, a') \in \mathbb{R}^2$  given by Proposition 3.10. On Figure 8, we have plotted, in the case  $h'(0) > 0$ , a control path  $(\gamma(t))_{t \in [0, 1]}$  which reaches the semi-conical intersection at  $t = t_0$ , following a first non-mixing curve for  $t \leq t_0$ , and such that  $\ddot{u}(t_0^-) = a$ . Then for  $t \geq t_0$ ,  $\gamma(t)$  follows the non-mixing curve whose second order derivative  $\ddot{\gamma}(t_0^+)$  is such that  $\ddot{u}(t_0^+) = a'$  (blue curve), so that it allows to reach the superposition of quantum states  $(p_1, p_2)$ , from an initial state  $\phi_1$ . In a second phase (green curve),  $\gamma(t)$  goes back to its initial point so as to design a loop, as it is required when designing adiabatic control strategies (see [8]).

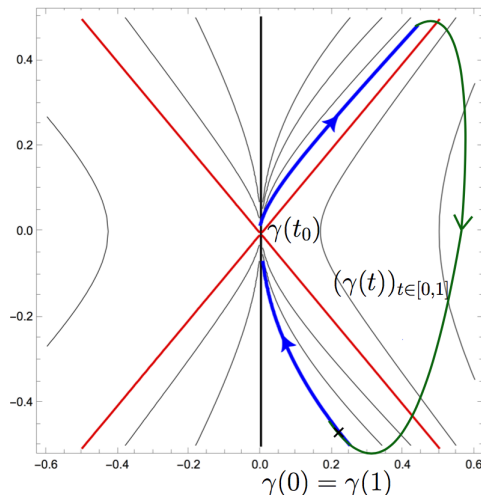


Figure 8: A control loop following the non-mixing curves having a second order discontinuity at the semi-conical singularity, in the plane of the controls  $(u, v) \in \mathbb{R}^2$ .

**Remark 3.11.** *If the aim is to induce complete transitions between the two quantum states at a semi-conical intersection, a suitable strategy is to design smooth paths passing through the semi-conical intersection in a direction which is transverse to the non-conical direction. An improvement*

of the strategy following the non-mixing curves is achievable in the hyperbolic case  $h'(0) > 0$ , while it is not in the elliptic case  $h'(0) < 0$ .

## 4 Classification of the singularities of the non-mixing field of a generic two-level system and its one-parameter bifurcations

The aim of this section is to prove, through the use of normal forms and a genericity study, the following two results which concern generic singularities of the non-mixing field for general two-level Hamiltonians

$$H_f = \begin{pmatrix} f_1 & f_2 \\ f_2 & -f_1 \end{pmatrix},$$

defined for  $f = (f_1, f_2) \in C^\infty(\mathbb{R}^2, \mathbb{R}^2)$  and  $f \in C^\infty(\mathbb{R}^3, \mathbb{R}^2)$ . The latter case corresponds to parametric families of two-level real Hamiltonians driven by two controls, and, in this case, the *parametric non-mixing field* is defined, for every  $z \in \mathbb{R}$ , as the non-mixing field associated with  $f(\cdot, \cdot, z)$ . It will be denoted as  $\chi_z(f)$ . In this setting, the definitions of conical and semi-conical intersections can be translated into conditions on the first and second order jets of  $f$  (see Appendix A.2 for more details).

The goal of this section is to prove the two next results, which provide a classification of the singularities of the non-mixing field for one parametric families of two-level systems.

**Theorem 4.1.** *Generically with respect to  $f \in C^\infty(\mathbb{R}^2, \mathbb{R}^2)$ ,  $\chi(f)$  has three types of singularities, up to a  $C^\infty$ -diffeomorphic coordinate change:*

- *Critical nodes at intersections of eigenvalues,*
- *Saddles and centers at points that are not intersections of eigenvalues.*

**Theorem 4.2.** *Generically with respect to  $f \in C^\infty(\mathbb{R}^3, \mathbb{R}^2)$ , for every  $z \in \mathbb{R}$ ,  $\chi_z(f)$  has the following singularities, up to a  $C^\infty$ -diffeomorphic coordinate change:*

- *Critical nodes at conical intersections of eigenvalues,*
- *Hyperbolic or elliptic semi-conical singularities at semi-conical intersections of eigenvalues,*
- *Saddles, centers or cusps at points that are not intersections of eigenvalues.*

In order to prove these two theorems, we need to recall the genericity results, admissible transformations of two-level Hamiltonians as introduced in [5] in order to find normal forms for semi-conical intersections. They can be found in Appendix A. Our proofs will be based on the following invariance result of the non-mixing field under the action of admissible transformations of Hamiltonians, which can be deduced easily from Proposition 3.2.

**Proposition 4.3.** *Let  $f, \tilde{f} \in C^\infty(\mathbb{R}^2, \mathbb{R}^2)$  (respectively,  $f, \tilde{f} \in C^\infty(\mathbb{R}^3, \mathbb{R}^2)$ ) be two equivalent functions, in the sense of Definition A.5 (respectively, Definition A.6). Then the regular non-mixing fields  $\chi(f)$  and  $\chi(\tilde{f})$  (respectively,  $\chi_z(f)$  and  $\chi_z(\tilde{f})$  for every parameter  $z \in [z_0, z_1]$ ) of  $f$  and  $\tilde{f}$  have diffeomorphic integral curves, that is, their corresponding non-mixing curves are diffeomorphic.*

### 4.1 Proof of Theorem 4.1

#### 4.1.1 Singularities of $\chi(f)$ at intersections of eigenvalues

First we study zeros of  $\chi(f)$  in the set  $\Sigma = \{(u, v) \in \mathbb{R}^2 \mid f_1(u, v) = f_2(u, v) = 0\}$ . We recall that generically w.r.t.  $f \in C^\infty(\mathbb{R}^2, \mathbb{R}^2)$  an intersection of eigenvalues is conical (see e.g [5, Section 2.1.1]).

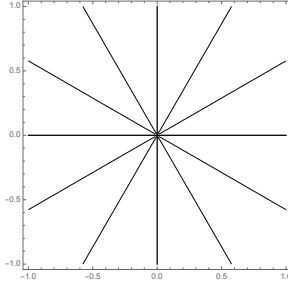


Figure 9: Non-mixing curves at a conical intersection.

Assume that  $H_f$  admits a conical intersection of eigenvalues at  $(0, 0)$ . The results of Appendix A.2.1 ensure that there exists a diffeomorphism  $\phi \in C^\infty(\mathbb{R}^2, \mathbb{R}^2)$  such that  $(f \circ \phi)(u, v) = (u, v)$  in a neighborhood of  $(0, 0)$ . Then the non-mixing curves of  $H_f$  are locally diffeomorphic to a critical node, that is, to the integral curves of the smooth vector field  $\mathbb{R}^2 \ni (u, v) \mapsto \begin{pmatrix} u \\ v \end{pmatrix}$  (see Figure 9).

#### 4.1.2 Other singularities of $\chi(f)$

Now we study the zeros of  $\chi(f)$  in the set  $\mathbb{R}^2 \setminus \Sigma$ . Without loss of generality, assume that  $(0, 0)$  is a zero of  $\chi(f)$  such that  $f_2(0) \neq 0$ . By definition of  $\chi(f)$  we obtain that  $(0, 0)$  is a critical point of  $g = \frac{f_1}{f_2}$ , which is  $C^\infty$  in a neighborhood of  $(0, 0)$ . By direct computations, we prove that the application  $\mathcal{F} : J^2(\mathbb{R}^2, \mathbb{R}^2) \rightarrow J^2(\mathbb{R}^2, \mathbb{R})$  such that  $\mathcal{F}(j^2(f)(0)) = j^2(g)(0)$  is a submersion, where for  $k \in \{1, 2\}$ ,  $J^2(\mathbb{R}^2, \mathbb{R}^k)$  is the space of 2-jets of functions from  $\mathbb{R}^2$  to  $\mathbb{R}^k$ , and for every  $(u, v) \in \mathbb{R}^2$  and  $f \in C^2(\mathbb{R}^2, \mathbb{R}^k)$ ,  $j^2(f)(u, v) \in J^2(\mathbb{R}^2, \mathbb{R}^k)$  denotes the 2-jet of  $f$  at  $(u, v)$ . Morse functions being open and dense in  $C^\infty(\mathbb{R}^2, \mathbb{R})$  (see [14, Theorem 6.2]), we deduce that generically with respect to  $f \in C^\infty(\mathbb{R}^2, \mathbb{R}^2)$ , the critical points of  $\chi(f)$  belonging to  $\mathbb{R}^2 \setminus \Sigma$  are saddles or centers, that is, the non-mixing curves are locally diffeomorphic to the integral curves of, respectively,  $(u, v) \mapsto \begin{pmatrix} u \\ -v \end{pmatrix}$ , or  $(u, v) \mapsto \begin{pmatrix} -v \\ u \end{pmatrix}$ .

## 4.2 Proof of Theorem 4.2

Let  $f = (f_1, f_2) \in C^\infty(\mathbb{R}^3, \mathbb{R}^2)$  and for every  $(u, v, z) \in \mathbb{R}^3$ ,

$$H_f(u, v, z) = \begin{pmatrix} f_1(u, v, z) & f_2(u, v, z) \\ f_2(u, v, z) & -f_1(u, v, z) \end{pmatrix}.$$

For every  $z$  in  $\mathbb{R}$ , let  $\chi_z(f)$  be the non-mixing field associated with  $f(\cdot, \cdot, z) \in C^\infty(\mathbb{R}^2, \mathbb{R}^2)$ .

### 4.2.1 Singularities of $\chi_z(f)$ at intersections of eigenvalues

Using the results of [2, Lemma 4.2.29], up to reducing the open and dense subset of  $C^\infty(\mathbb{R}^3, \mathbb{R}^2)$  to which  $f$  belongs, we can prove that

**Proposition 4.4.** *Generically w.r.t.  $f \in C^\infty(\mathbb{R}^3, \mathbb{R}^2)$ ,  $H_f(\cdot, \cdot, 0)$  is equivalent to*

$$H(u, v) = \begin{pmatrix} uh(u) & u + v^2 \\ u + v^2 & -uh(u) \end{pmatrix} \quad (10)$$

where  $h : \mathbb{R} \rightarrow \mathbb{R}$  is a smooth function such that  $h(0) = 1$  and  $h'(0) \neq 0$ .

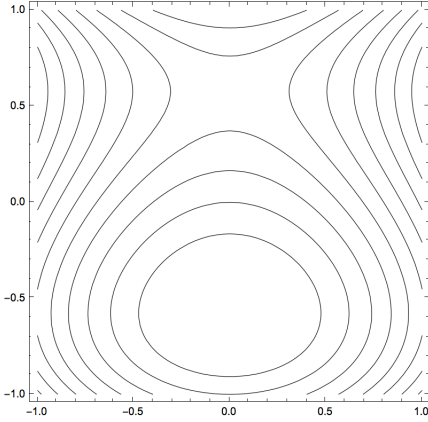


Figure 10: Saddle-center bifurcation for  $z < \bar{z}$ ,  $\bar{z}$  being the value of  $z$  for which the bifurcation occurs.

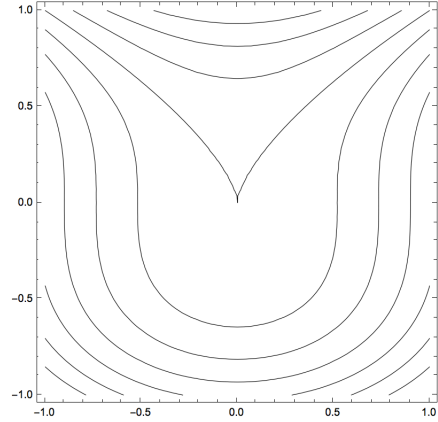


Figure 11: Saddle-center bifurcation for  $z = \bar{z}$ .

Hence we can deduce the two first claims of the theorem.

#### 4.2.2 Singularities of $\chi_z(f)$ at other points

We present the next lemma, which is classical and can be deduced from [21, §4.3].

**Lemma 4.5.** *For  $g \in C^\infty(\mathbb{R}^3, \mathbb{R})$ , we define, for every  $(u, v) \in \mathbb{R}^2$ ,  $g_z(u, v) = g(u, v, z)$ . Generically with respect to  $g \in C^\infty(\mathbb{R}^3, \mathbb{R})$ , for every  $z \in \mathbb{R}$ , the critical points of  $g_z$  are such that the level-lines of  $g_z$  are locally diffeomorphic to a saddle, a center as in Proposition 4.1.2, or a cusp, that is the level lines of  $(u, v) \mapsto v^3 - u^2$ .*

More precisely, the cusp singularity is obtained by a *saddle-center bifurcation*, that is  $g_z(u, v) = v^3 \pm (z - \bar{z})v - u^2$ , the bifurcation occurs for a value of the parameter  $z = \bar{z}$  (see [21, §4.3]), and it is illustrated on the Figures 10 and 11.

**Remark 4.6.** *Semi-conical singularities and cusps are singularities of maximal codimension. Hence, generically, we cannot find them simultaneously for the same value of the parameter  $z$ .*

### 4.3 An avoided crossing model obtained for parametric families having semi-conical intersections

Set  $n \geq 2$  and consider a family  $(H_z(u, v))_{z \in \mathbb{R}}$  of  $n \times n$  real symmetric matrices such that  $(u, v, z) \mapsto H_z(u, v)$  is  $C^\infty$ . Assume that, for  $z > 0$ ,  $H_z$  has simple eigenvalues and  $H_0$  has an isolated double eigenvalue at  $(u, v) = (\bar{u}, \bar{v})$ . It results from the structural stability of conical intersections for a real Hamiltonian with two real controls (see [8]) that  $(\bar{u}, \bar{v})$  is a non-conical intersection for  $H_0(\bar{u}, \bar{v})$ . In this case, the family  $(H_z(\cdot))_{z \in \mathbb{R}}$  is said to have an *avoided crossing* at  $(0, 0)$  (see [18, 19, 20] for results about the use of avoided crossings in semi-classical analysis), in the sense of the definition adapted from [19], as follows.

**Definition 4.7.** *Assume that  $H_z$  is a family of self adjoint operators on a Hilbert space  $\mathcal{H}$ , depending smoothly on a control  $u \in \mathbb{R}^k$ ,  $k \geq 1$  and on a parameter  $z \in \mathbb{R}$ . Assume that there exist two eigenvalues  $\lambda_1^z$  and  $\lambda_2^z$  separated from the rest of the spectrum of  $H_z(u)$  for every  $u$  in a compact set  $K$  of  $\mathbb{R}^k$  and  $z \in [-z_0, z_0]$ , where  $z_0 > 0$ . Assume  $\Gamma = \{u \mid \lambda_1^0(u) = \lambda_2^0(u)\}$  is a single point or a non-empty connected proper submanifold of  $\mathbb{R}^k$  and that for every  $u \in K$ ,  $\lambda_1^z(u) \neq \lambda_2^z(u)$  for  $z > 0$ . Then we say that  $H_z(u)$  has an avoided crossing on  $\Gamma$ .*



### 4.3.1 Semi-conical avoided crossing

We have shown in [5] that semi-conical intersections of eigenvalues are obtained by generic parametric bifurcation of real Hamiltonians driven by two controls  $k = 2$ . Furthermore, considering real Hamiltonians with two control parameters  $k = 2$  and assuming that  $\Gamma$  is reduced to a point, it is easy to see that such model corresponds to the least degenerate model of avoided crossing.

More precisely, by the results of [5, Section 6] associated with [5, Theorem 2.14] the study of such  $n \times n$  Hamiltonian  $H_z$  can be reduced locally to the study of a two-level Hamiltonian which is equivalent, in the sense of Definition A.6 to the two-level Hamiltonian

$$\tilde{H}_z(u, v) = \begin{pmatrix} h_1(u, v, z)(z - m(u)u) & h_2(u, v, z)(z + u + v^2) \\ h_2(u, v, z)(z + u + v^2) & -h_1(u, v, z)(z - m(u)u) \end{pmatrix}$$

for every  $(u, v, z)$  in a neighborhood of  $(0, 0, 0)$ , where  $h_1, h_2 \in C^\infty(\mathbb{R}^3, \mathbb{R}^2)$  satisfy  $h_1(0) = h_2(0) = 1$  and  $m \in C^\infty(\mathbb{R}, \mathbb{R})$  satisfies  $m(0) \neq 0$ ,  $m(0) > -1$ .

To the best of the author's knowledge, such a model has not been studied yet. Indeed, this case has not been exposed in [19], especially because in the latter, the author considers only avoided crossings corresponding to eigenvalue intersections that can be obtained generically in the space of Hamiltonians depending on  $u \in \mathbb{R}^k$ , while in this article we are considering genericity w.r.t. Hamiltonians depending on  $(u, z) \in \mathbb{R}^k \times \mathbb{R}$ . Our model possesses the following qualitative properties, which are illustrated on Figure 12:

- For  $z < 0$ , the energy levels have two conical intersections.
- For  $z \rightarrow 0$  and  $z < 0$ , these two singular points join along the non-conical direction, their common limit point is a semi-conical intersection.
- For  $z > 0$ , the energy levels are separated.

In accordance with the results of Section 3, the case where  $h'(0) > 0$  is referred as the *Hyperbolic bifurcation*, and the case where  $h'(0) < 0$  is referred as the *Elliptic bifurcation*. We can show that the condition  $h'(0) \neq 0$  is satisfied when the functions  $(h_1, h_2, m)$  are such that  $-4\partial_1 \tilde{h}(0, 0, 0)\tilde{h}(0, 0, 0) \neq \partial_2 \tilde{h}(0, 0, 0)^2$ , where for every  $(u, v, z)$  in a neighborhood of 0 in  $\mathbb{R}^3$ ,  $\tilde{h}(u, v, z) = -\frac{h_1(u, v, z)m(u)}{h_2(u, v, z)}$ . Thanks to Proposition 4.4, we prove that such property holds generically.

### 4.3.2 Use of the non-mixing curves for two-level systems

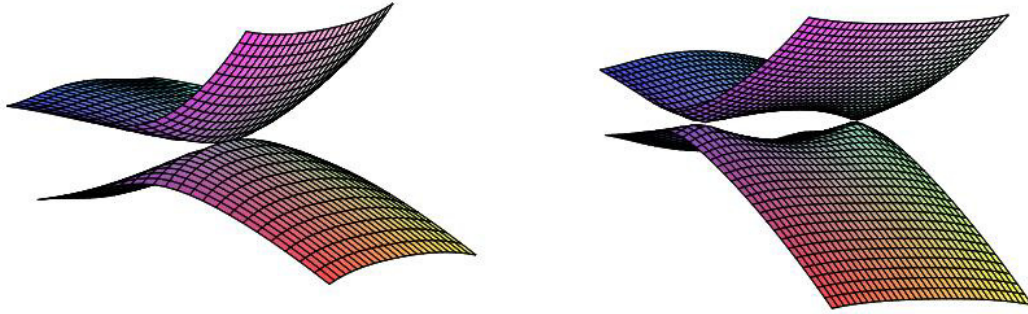
We propose here to study the non-mixing curves associated with  $\tilde{H}_z$ , that corresponds to a Hamiltonian  $H_f$  with  $f = (f_1, f_2) \in C^\infty(\mathbb{R}^3, \mathbb{R}^2)$  where  $f_1(u, v, z) = h_1(u, v, z)(z - m(u)u)$  and  $f_2(u, v, z) = h_2(u, v, z)(z + u + v^2)$ . This Hamiltonian provides the behavior of general two-level systems having Elliptic or Hyperbolic semi-conical bifurcations. Notice that the definition of semi-conical intersections and bifurcations are not exclusive to two-level systems, so that the methodology could be used also for more general quantum systems, and in this case we can conjecture that the non-mixing curves have the same singularities as those obtained for two-level systems. Under these assumptions, by Section 3, the non-mixing field  $\chi_0(f)$  of  $\tilde{H}_0$  has an elliptic or hyperbolic semi-conical singularity at  $(0, 0)$ , as plotted on the figures 3 and 4. Assuming  $m(0) > -1$ , we obtain that for  $z > 0$  (respectively,  $z < 0$ ),  $\tilde{H}_z$  has no intersection of eigenvalues, and that for  $z < 0$  (respectively  $z > 0$ ),  $\tilde{H}_z$  has two conical intersections of eigenvalues.

For  $z < 0$  (see Figures 13 and 14), the non-mixing curves are the integral curves of a smooth vector field vanishing at each conical intersections which has an index equal to 1 at conical intersections, and by Section 3,  $\chi_z(f)$  has critical nodes at these points. In the hyperbolic case  $h'(0) > 0$ , the two critical nodes (of index +1) are combined with two saddles (of index -1). By a continuity argument

of the index with respect to the parameter  $z$ , this is coherent with the fact that the index of the hyperbolic semi-conical singularity vanishes. In the elliptic case  $h'(0) < 0$ , the two critical nodes join in the non-conical direction and there is no other singularity in a neighborhood of 0. For  $z = 0$  (see Figures 3 and 4) the singularity that we obtain is the semi-conical elliptic or hyperbolic singularity (see Section 3) and has an index either equal to 2 in the elliptic case or 0 in the hyperbolic case.

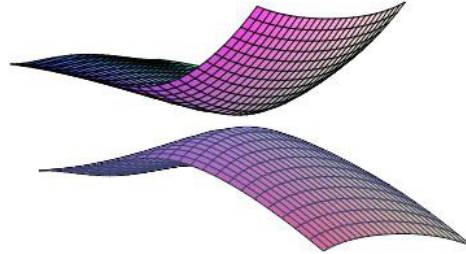
For  $z > 0$  (see Figures 15 and 16), the non-mixing curves are the integral curves of a smooth vector field which is non-singular at 0.

For  $z \rightarrow 0$ , the direction of the non-mixing curves at 0 converges to the non-conical direction of  $\tilde{H}_0$ . In the elliptic case, however, there are two center singularities in a neighborhood of the origin. By a continuity argument of the index w.r.t.  $z$ , this is coherent with the fact that the index of the elliptic semi-conical singularity is equal to 2.



(a) Energy levels of  $\tilde{H}^0(u, v)$ .

(b) Energy levels of  $\tilde{H}^z(u, v)$  with  $z < 0$ .



(c) Energy levels of  $\tilde{H}^z(u, v)$  with  $z > 0$ .

Figure 12: Avoided-crossing in the semi-conical intersection model: the submanifold  $\Gamma$  is reduced to a point, and  $k = 2$ .

In a general setting of avoided crossing, one can question the possibility of guaranteeing the system to stay on a given state with higher precision when  $z > 0$  is small, that is, when the two eigenvalue

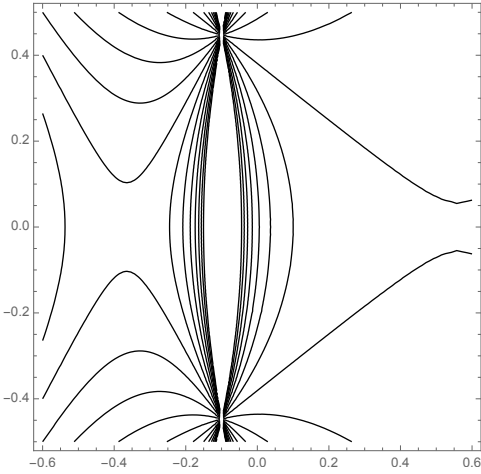


Figure 13: Hyperbolic non-mixing curves for  $z < 0$ .

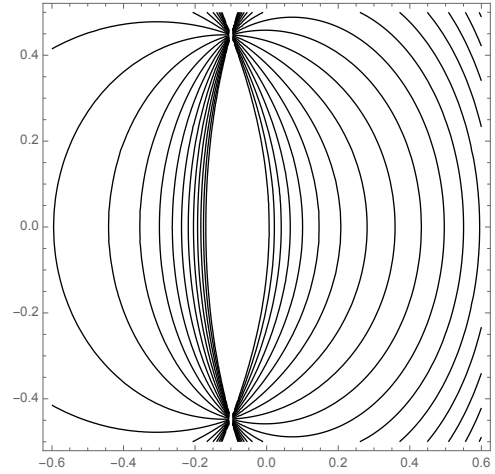


Figure 14: Elliptic non-mixing curves for  $z < 0$ .

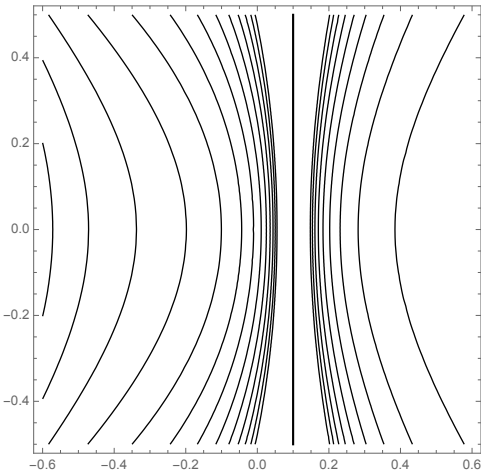


Figure 15: Hyperbolic non-mixing curves for  $z > 0$ .

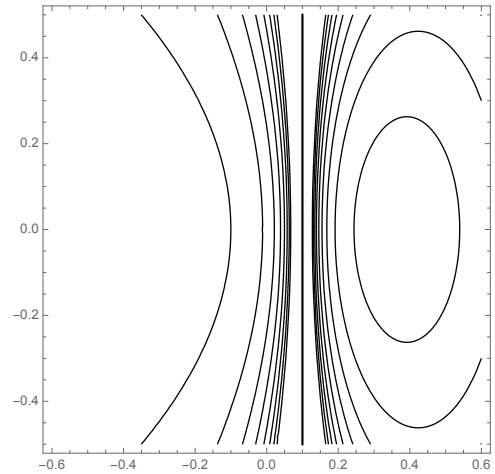


Figure 16: Elliptic non-mixing curves for  $z > 0$ .

surfaces are very close to each other so that undesirable transitions may appear if the speed along the control path is not small enough. For semi-conical intersections, a possible way to tackle this issue is to follow the non-mixing curves, which are represented on the figures 15 and 16. For a very small  $z > 0$ , one could be interested in ensuring that the system remains on the lower energy level. In order to achieve such a task, we propose to consider control paths which follow the non-mixing curves, then reducing the possible losses to the higher energy level, which depend usually on the inverse of the gap between the two levels (see for instance [26, Theorem 2.2]).

## 5 The non-mixing field for general quantum systems without the separation condition (GAP)

Consider, as in Section 2, an operator  $H$  on a separable Hilbert space  $\mathcal{H}$  satisfying Assumption  $(\mathcal{R})$ . The aim of this section is to understand the behavior of the non-mixing field  $\chi_{j-1,j}$  between two eigenvalues  $\lambda_{j-1}$  and  $\lambda_j$  of  $H$ , when the separation condition **(GAP)** of the part  $\{\lambda_{j-1}(u), \lambda_j(u)\}$  of

the spectrum of  $H(u)$  that was made in Section 2 is violated at some isolated point  $u \in \mathbb{R}^2$ . In order to tackle this case, we assume that the following holds:  $\sigma_*(u) = \{\lambda_{j-1}(u), \lambda_j(u), \lambda_{j+1}(u)\} \subset \sigma(u)$  is a locally discrete separated part of the spectrum  $\sigma(u)$  of  $H(u)$ , for every  $u \in U$ . Assuming that there exists  $(\bar{u}, \bar{v}) \in \mathbb{R}^2$  such that  $\lambda_j(\bar{u}, \bar{v}) = \lambda_{j+1}(\bar{u}, \bar{v})$ , the goal is to understand the behavior of the integral curves of  $\chi_{j-1,j}$  in a neighborhood of  $(\bar{u}, \bar{v})$ . While  $\chi_{j-1,j}$  can be locally identified with a smooth vector field when the separation condition is satisfied (see Section 2.2), this is no more the case when the latter is violated. The main result of this section, which is stated in Theorem 5.1 proves that, under suitable conditions on  $H$ , the non-mixing field  $\chi_{j-1,j}$  admits a Darbouxian singularity at  $(\bar{u}, \bar{v})$ . Darbouxian singularities, which are defined in Appendix B, are classical examples of half-integer index singularities (see the figures 23, 24, and 25).

Assume that for every  $(u, v) \in U \setminus \{(\bar{u}, \bar{v})\}$ ,  $\lambda_j(u, v) \notin \{\lambda_{j+1}(u, v), \lambda_{j-1}(u, v)\}$ . For every  $(u, v) \in U$  and  $k \in \{j, j+1\}$ , let  $P_{k-1,k}(u, v) : \mathbb{R}^n \rightarrow \mathbb{R}^n$  be the orthogonal projection of  $H(u, v)$  onto the eigenspace associated with  $\lambda_{k-1}(u, v)$  and  $\lambda_k(u, v)$ , which is smooth with respect to  $(u, v) \in U$ . As in [5, Section 6], for every  $(u, v) \in U$ , define an orthogonal map  $I_{k-1,k}(u, v) : \mathbb{R}^2 \rightarrow \text{Im}P_{k-1,k}(u, v)$ , smoothly depending on  $(u, v)$ . For  $k \in \{j, j+1\}$ , consider a normalized real eigenvector  $\phi_k(u, v)$  (respectively,  $\phi_{k+1}(u, v)$ ) of  $H(u, v)$  associated with  $\lambda_k(u, v)$  (respectively,  $\lambda_{k+1}(u, v)$ ). Define the two-level Hamiltonian  $h(u, v) = I_{j,j+1}^{-1}(u, v)H(u, v)I_{j,j+1}(u, v)$ , and normalized real eigenvector  $\tilde{\phi}_j(u, v)$  (respectively,  $\tilde{\phi}_{j+1}(u, v)$ ) of  $h_{\text{red}}(u, v)$  associated with  $\lambda_k(u, v)$  (respectively,  $\lambda_{k+1}(u, v)$ ), where the two-level Hamiltonian  $h_{\text{red}}(u, v)$  is obtained by removing the trace of  $h(u, v)$ . Notice that we have  $I_{j,j+1}(u, v)(\tilde{\phi}_j(u, v)) = \eta\phi_j(u, v)$ , where  $\eta = \pm 1$ .

The main result of this section is the following. It states that  $\chi_{j-1,j}$  has Darbouxian line field singularities at conical intersections  $(\bar{u}, \bar{v})$  of eigenvalues between  $\lambda_j$  and  $\lambda_{j+1}$  under the following condition:

**Condition (C):** The vectors  $P_{j,j+1}H_1\phi_{j-1}(\bar{u}, \bar{v})$  and  $P_{j,j+1}H_2\phi_{j-1}(\bar{u}, \bar{v})$  are not colinear.

**Theorem 5.1.** *Let  $(\bar{u}, \bar{v}) \in \mathbb{R}^2$  be such that  $\lambda_j(\bar{u}, \bar{v}) = \lambda_{j+1}(\bar{u}, \bar{v})$  is a conical intersection. Assume that Condition (C) is satisfied at  $(\bar{u}, \bar{v})$ . Then  $\chi_{j-1,j}$  has a Darbouxian singularity at  $(\bar{u}, \bar{v})$ .*

In order to prove Theorem 5.1, we will take advantage of the methods developed in [7], where the authors defined a particular topology on line fields thanks to the angular bisection of pairs of smooth vector fields. In particular, they defined Hyperbolic singularities of line fields and showed that they correspond to Darbouxian singularities, up to homeomorphic transformations. The main step of the proof is the successive application of the theorems 5.3 and B.9 which can be found in Appendix B.

## 5.1 Proof of Theorem 5.1

We start by proving the following result concerning two-level systems. We refer to Appendix B for notations.

**Proposition 5.2.** • *Let  $f = (f_1, f_2) \in C^\infty(\mathbb{R}^2, \mathbb{R}^2)$ ,  $H_f = \begin{pmatrix} f_1 & f_2 \\ f_2 & -f_1 \end{pmatrix}$ , and  $g$  be the Euclidean metric on  $\mathbb{R}^2$ . Then the real eigendirections of  $h_f$  associated with the eigenvalues  $\lambda_\pm = \pm\sqrt{f_1^2 + f_2^2}$  can be written as the line-fields  $L_- = B_g\left(\begin{pmatrix} -f_2 \\ f_1 \end{pmatrix}, \begin{pmatrix} 0 \\ 1 \end{pmatrix}\right)$ , and  $L_+ = B_g\left(\begin{pmatrix} -f_2 \\ f_1 \end{pmatrix}, \begin{pmatrix} 0 \\ -1 \end{pmatrix}\right)$ . Assume moreover that  $f$  has a conical intersection at 0, that is,  $f(0) = 0$  and  $Df(0) \in GL_2(\mathbb{R})$ . Then the proto-line-fields  $\left(\begin{pmatrix} -f_2 \\ f_1 \end{pmatrix}, \begin{pmatrix} 0 \\ 1 \end{pmatrix}\right)$  and  $\left(\begin{pmatrix} -f_2 \\ f_1 \end{pmatrix}, \begin{pmatrix} 0 \\ -1 \end{pmatrix}\right)$  have non-degenerate singularities at 0.*

- Let  $f = (f_1, f_2, f_3) \in C^\infty(\mathbb{R}^2, \mathbb{R}^3)$  and  $M_f = \begin{pmatrix} f_1 & f_2 \\ f_2 & f_3 \end{pmatrix}$ . Define  $\tilde{f} \in C^\infty(\mathbb{R}^2, \mathbb{R}^2)$  as  $\tilde{f} = (\frac{f_1 - f_3}{2}, f_2)$ . Then the real eigendirections of  $M_f$  are those of  $H_{\tilde{f}}$ . Moreover  $M_f$  has a conical intersection at 0 if and only if  $H_{\tilde{f}}$  has a conical intersection at 0.

*Proof.* Let  $(\bar{u}, \bar{v}) \in \mathbb{R}^2$  be such that  $f(\bar{u}, \bar{v}) \neq 0$ . By direct computations,  $\begin{pmatrix} x \\ y \end{pmatrix} \in \mathbb{R}^2$  is an eigenvector of  $H_f(u, v)$  associated with  $\lambda_\pm(u, v)$  if and only if  $x(f_1(u, v) - \lambda_\pm(u, v)) + yf_2(u, v) = 0$ , that is,  $\begin{pmatrix} x \\ y \end{pmatrix}$  is colinear to  $\frac{1}{\lambda_\pm(u, v)} \begin{pmatrix} -f_2(u, v) \\ f_1(u, v) \end{pmatrix} + \begin{pmatrix} 0 \\ -1 \end{pmatrix}$ . Define the vector field  $X$ , for every  $(u, v) \in \mathbb{R}^2$ , by  $X(u, v) = \begin{pmatrix} -f_2(u, v) \\ f_1(u, v) \end{pmatrix}$ . The hypothesis that 0 is a conical intersection for  $f$  yields that  $X(0) = 0$  and  $DX(0)$  is non-degenerate. The first claim is proved, and the second claim is obtained by direct computations.  $\square$

**Proposition 5.3.** *There exists  $A \in C^\infty(\mathbb{R}^2, M_2(\mathbb{R}))$  such that, for every  $(u, v) \in U \setminus \{(\bar{u}, \bar{v})\}$ ,  $\chi_{j-1, j}(u, v)$  defines the same direction as  $A(u, v)\tilde{\phi}_j(u, v)$ .*

*Proof.* Consider a smooth vector field  $X$  on  $\mathbb{R}^2$  such that, for every  $(u, v) \in U$ ,  $I_{j, j+1}(u, v)(X(u, v)) = P_{j, j+1}(u, v)(H_2\phi_{j-1}(u, v))$ , and a smooth vector field  $Y$  on  $\mathbb{R}^2$  such that, for every  $(u, v) \in U$ ,  $I_{j, j+1}(u, v)(Y(u, v)) = -P_{j, j+1}(u, v)(H_1\phi_{j-1}(u, v))$ . Notice that the smoothness of  $X$  and  $Y$  rely on the fact that  $\phi_{j-1}(u, v)$  can be chosen smooth with respect to  $(u, v) \in U$ . Denoting by  $g$  the Euclidean scalar product on  $\mathbb{R}^2$ , we can write

$$\begin{aligned} \langle H_2\phi_{j-1}(u, v), \phi_j(u, v) \rangle &= \langle H_2\phi_{j-1}(u, v), \eta I_{j, j+1}(u, v)(\tilde{\phi}_j(u, v)) \rangle \\ &= \eta \langle P_{j, j+1}(u, v)(H_2\phi_{j-1}(u, v)), I_{j, j+1}(u, v)(\tilde{\phi}_j(u, v)) \rangle \\ &= \eta \langle I_{j, j+1}(u, v)(X(u, v)), I_{j, j+1}(u, v)(\tilde{\phi}_j(u, v)) \rangle \\ &= \eta g(X(u, v), \tilde{\phi}_j(u, v)), \end{aligned}$$

where the last equality is obtained using that  $I_{j, j+1}(u, v)$  is an orthogonal map between  $\mathbb{R}^2$  and  $\text{Im}P_{j, j+1}(u, v)$ , for every  $(u, v) \in U$ . By the same computations, we have  $-\langle H_1\phi_{j-1}(u, v), \phi_j(u, v) \rangle = \eta g(Y(u, v), \tilde{\phi}_j(u, v))$ . Denoting the coordinates of  $X$  and  $Y$  in the canonical basis of  $\mathbb{R}^2$  by  $X(u, v) = \begin{pmatrix} x_1(u, v) \\ x_2(u, v) \end{pmatrix}$  and  $Y(u, v) = \begin{pmatrix} y_1(u, v) \\ y_2(u, v) \end{pmatrix}$ , we have, by Proposition 2.4, for every  $(u, v) \in U \setminus \{(\bar{u}, \bar{v})\}$ ,

$\chi_{j-1, j}(u, v) = \eta A(u, v)\tilde{\phi}_j(u, v)$ , where, for every  $(u, v) \in U$ ,  $A(u, v) = \begin{pmatrix} x_1(u, v) & x_2(u, v) \\ y_1(u, v) & y_2(u, v) \end{pmatrix}$ , and  $\eta = \pm 1$ . We deduce the result.  $\square$

We can conclude the proof of Theorem 5.1.

*Proof of Theorem 5.1.* By definition  $\tilde{\phi}_j$  is the eigendirection associated with the eigenvalue  $\lambda_j$  of the two-level Hamiltonian  $h_{\text{red}}$  having a conical intersection at  $(\bar{u}, \bar{v})$ . Hence Proposition 5.2 proves that the line field  $\tilde{\phi}_j$  has a non-degenerate singularity at  $(\bar{u}, \bar{v})$ . Under assumption **(C)**, the matrix  $A \in C^\infty(\mathbb{R}^2, M_2(\mathbb{R}))$  defined in Proposition 5.3 is invertible. By Proposition B.9, we deduce that  $\chi_{j-1, j} = A\tilde{\phi}_j$  (where the equality is defined as the equality of the associated directions in  $\mathbb{R}^2$ ) has a non-degenerate singularity at  $(\bar{u}, \bar{v})$ . We deduce the theorem by using Proposition B.8.  $\square$

## 6 The non-mixing field in classical cases

### 6.1 Example 1: STIRAP processes

Consider the three-level system with controlled Hamiltonian  $H(u, v) = \begin{pmatrix} E_1 & u & 0 \\ u & E_2 & v \\ 0 & v & E_3 \end{pmatrix}$ , for  $E_1, E_2, E_3 \in \mathbb{R}$ .

In particular, we propose to illustrate the fact that the controlled parametric Hamiltonian

$H_z(u, v) = \begin{pmatrix} z & u & 0 \\ u & E_2 & v \\ 0 & v & E_3 \end{pmatrix}$ , for  $z, E_2, E_3 \in \mathbb{R}$  possesses a semi-conical avoided crossing at  $z = E_2$ ,

in the sense developed in Section 4.3. Note that, in accordance with the results of [3, Section 3.3], this model (or the multilevel Stirap in higher dimension) has utter importance, provided that under suitable non resonance assumptions, every finite dimensional single control system can be approximated in the adiabatic regime by a similar two control system in the Rotating Wave Approximation framework.

#### 6.1.1 Case where $E_1 < E_2 < E_3$

This case provides an example of system whose non-mixing field between two successive levels has both Darbouxian singularities (see, Section 5) and Type **(N)** node singularities (see, Section 2.2). We can prove the following result, which is illustrated on the figures 17 and 20.

**Proposition 6.1.** *The non-mixing field  $\chi_{1,2}$  (respectively  $\chi_{2,3}$ ) of  $H$  has:*

- *Type **(N)** node singularities at the points  $(u, v) \in \mathbb{R}^2$  such that  $\lambda_1(u, v) = \lambda_2(u, v)$  (respectively,  $\lambda_2(u, v) = \lambda_3(u, v)$ ) that are*

$$(u, v) = (0, \pm\sqrt{(E_1 - E_3)(E_1 - E_2)}) \left( \text{respectively } (\pm\sqrt{(E_1 - E_3)(E_2 - E_3)}, 0) \right).$$

- *Darbouxian singularities at the points  $(u, v) \in \mathbb{R}^2$  such that  $\lambda_2(u, v) = \lambda_3(u, v)$  (respectively,  $\lambda_1(u, v) = \lambda_2(u, v)$ ) that are*

$$(u, v) = (\pm\sqrt{(E_1 - E_3)(E_2 - E_3)}, 0) \left( \text{respectively } (0, \pm\sqrt{(E_1 - E_3)(E_1 - E_2)}) \right).$$

*Proof.* It is a classical fact that the points

$$(u, v) = (0, \pm\sqrt{(E_1 - E_3)(E_1 - E_2)})$$

are conical intersections between  $\lambda_1$  and  $\lambda_2$ , while the points

$$(u, v) = (\pm\sqrt{(E_1 - E_3)(E_2 - E_3)}, 0)$$

are conical intersections between  $\lambda_2$  and  $\lambda_3$  (this fact can be proved easily by checking the conditions on the conicity matrix exposed in [8, Proposition 4.4]). The first point can be deduced using the results exposed in Section 2.2.

Moreover, we show without difficulty that Condition **(C)** is satisfied at such points. Indeed, on the line  $v = 0$ , we have for every  $u \in \mathbb{R}$ ,  $\langle \phi_1(u, 0), e_3 \rangle = 0$ , and up to a reordering between  $\phi_2$  and  $\phi_3$ , we obtain  $\langle \phi_2(u, 0), e_3 \rangle = 0$  and  $\langle \phi_3(u, 0), e_1 \rangle = \langle \phi_3(u, 0), e_2 \rangle = 0$ . Hence  $\text{span}(P_{23}(u, 0))$  is a

plane of  $\mathbb{R}^3$  which is orthogonal to  $\text{span}(e_1, e_2)$  for every  $u \in \mathbb{R}$ . Considering  $H_1 = \begin{pmatrix} 0 & 1 & 0 \\ 1 & 0 & 0 \\ 0 & 0 & 0 \end{pmatrix}$ , and

$H_2 = \begin{pmatrix} 0 & 0 & 0 \\ 0 & 0 & 1 \\ 0 & 1 & 0 \end{pmatrix}$ , we can deduce that  $P_{23}(\bar{u}, 0)H_2\phi_1(\bar{u}, 0) \in \text{Span}(e_3) \setminus \{0\}$  and  $P_{23}(\bar{u}, 0)H_1\phi_1(\bar{u}, 0) \in \text{Span}(e_1, e_2) \setminus \{0\}$ , where  $\bar{u} = \pm\sqrt{(E_1 - E_3)(E_2 - E_3)}$ . We conclude by applying Theorem 5.1. The same reasoning applies to the points  $(0, \pm\sqrt{(E_1 - E_3)(E_1 - E_2)})$ . □

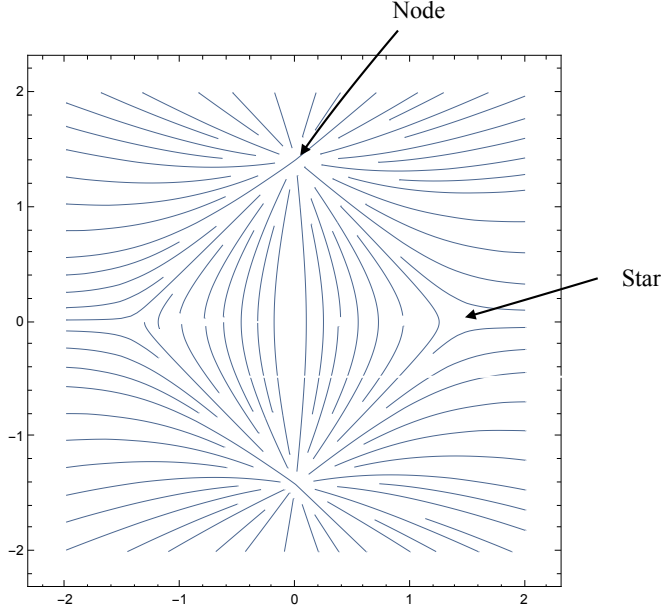


Figure 17: Non-mixing field between  $\lambda_1$  and  $\lambda_2$  for the STIRAP of Corollary 6.1.

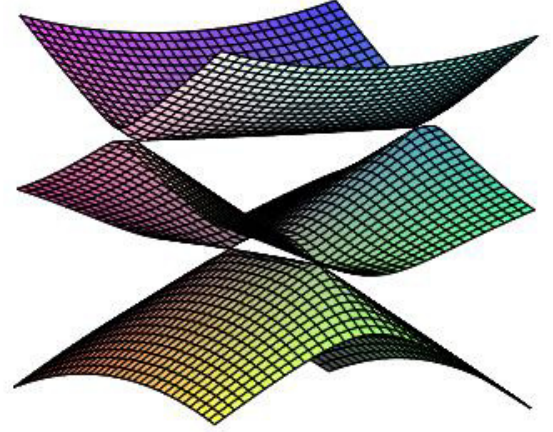


Figure 18: Spectrum as a function of  $(u, v)$  for the STIRAP, where  $E_1 < E_2 < E_3$ .

On Figure 17, we have plotted the non-mixing curves between the levels  $\lambda_1$  and  $\lambda_2$  when  $E_1 < E_2 < E_3$ . Along these curves the precision of the adiabatic approximation for a regular control path at speed  $\epsilon$  has an order equal to  $O(\epsilon)$  on a time interval of length  $\frac{1}{\epsilon}$ . In particular, those curves allow to induce transitions of states between the first and second levels passing at the node singularity along an integral curve of  $\chi_{12}$ , and, more generally, they allow to suppress the direct losses between those levels in the adiabatic regime, which can be of utter importance in practical implementations.

### 6.1.2 Semi-conical bifurcation: $E_1 = E_2 < E_3$ and $E_2 < E_1 < E_3$ .

When considering the case where  $E_1 = E_2 < E_3$ , we can prove that the system admits two conical intersections between the levels  $\lambda_2$  and  $\lambda_3$  at the points

$$(u, v) = (\pm\sqrt{(E_1 - E_3)(E_2 - E_3)}, 0) = (\pm|E_1 - E_3|, 0),$$

at which Condition (C) is not satisfied, and we can check on numerical examples that there is a semi-conical intersection between the levels  $\lambda_1$  and  $\lambda_2$  at  $(0, 0)$ . On Figure 19, we have plotted the non-mixing curves between the levels  $\lambda_1$  and  $\lambda_2$  in this case. We observe that the non-mixing field

$\chi_{12}$  between the levels  $\lambda_1$  and  $\lambda_2$  is non-singular at the points  $(\pm|E_1 - E_3|, 0)$ , and that there is a node singularity at the semi-conical intersection  $(0, 0)$  between the levels  $\lambda_1$  and  $\lambda_2$ .

In further studies, it would be interesting to prove rigorously that the singularity at the origin is a node, by studying the non-mixing field at a semi-conical intersection for  $n$ -level systems with  $n \geq 2$ . The non-mixing field of the considered three level STIRAP system seems to be represented at the origin by a two-level system having a semi-conical intersection that can be turned into the normal form of Definition 3.4 such that the function  $h$  satisfies  $h'(0) = 0$ . Hence the fact that we obtain a slightly different singularity from the elliptic and hyperbolic cases studied in Section 4 is not surprising.

When considering the case where  $E_2 < E_1 < E_3$ , we can prove that the system admits two conical intersections between the levels  $\lambda_2$  and  $\lambda_3$  at the points  $(u, v) = (\pm\sqrt{(E_1 - E_3)(E_2 - E_3)}, 0)$ , at which Condition (C) is satisfied, and admits no intersection between the levels  $\lambda_1$  and  $\lambda_2$ . As a consequence, the non-mixing field  $\chi_{12}$  between the levels  $\lambda_1$  and  $\lambda_2$  has Darbouxian singularities at the points  $(\pm\sqrt{(E_1 - E_3)(E_2 - E_3)}, 0)$ . On Figure 21, we have plotted the non-mixing curves between the levels  $\lambda_1$  and  $\lambda_2$  in this case. We notice the presence of Lemon singularities at the points  $(u, v) = (\pm\sqrt{(E_1 - E_3)(E_2 - E_3)}, 0)$ .

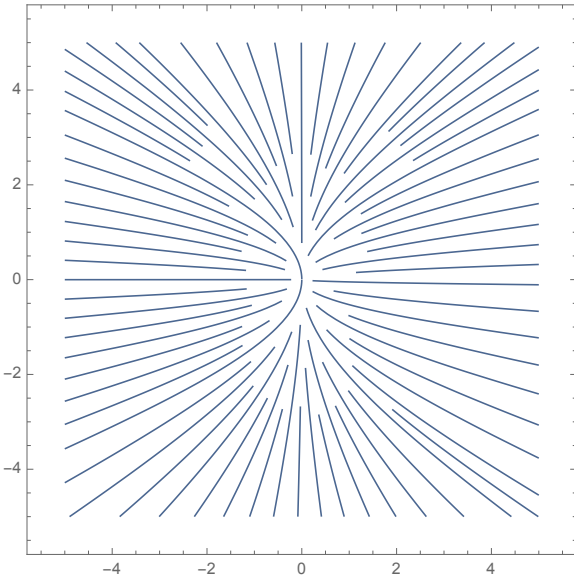


Figure 19: Non-mixing field between  $\lambda_1$  and  $\lambda_2$  for the degenerate STIRAP, where  $E_1 = E_2 < E_3$ .

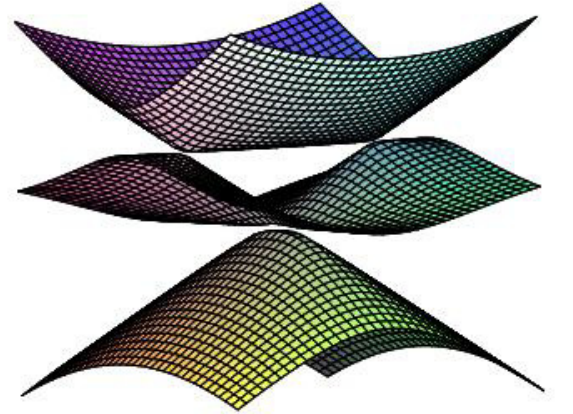


Figure 20: Spectrum as a function of  $(u, v)$  for the degenerate STIRAP, where  $E_1 = E_2 < E_3$ .

## 6.2 Example 2: Eberly-Law models

We can show that the previous results about STIRAP processes can be extended to some models of coupled spin-oscillator dynamics (see [22, 29, 6]), which are represented by the infinite-dimensional controlled quantum system on a separable Hilbert space  $\mathcal{H}$

$$i \frac{d\psi(t)}{dt} = H(u, v)\psi, \quad \psi(t) \in \mathcal{H},$$



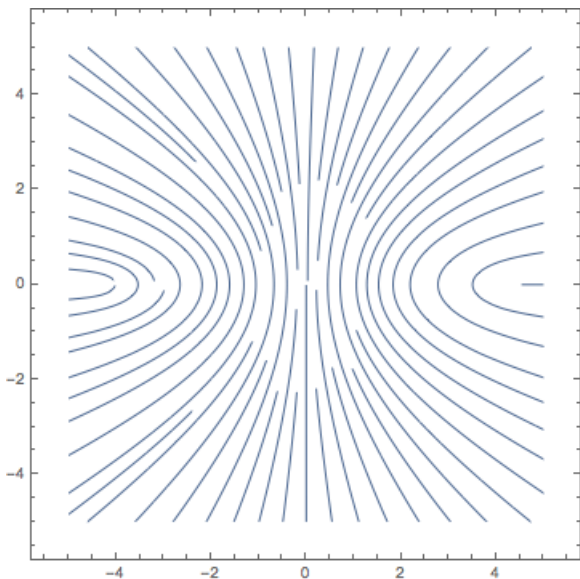


Figure 21: Non-mixing field between  $\lambda_1$  and  $\lambda_2$  for the STIRAP, where  $E_2 < E_1 < E_3$ .

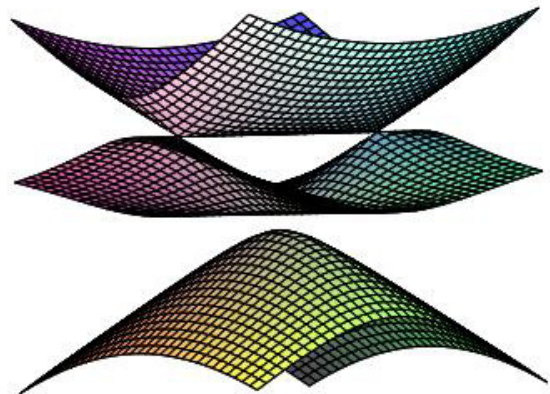


Figure 22: Spectrum as a function of  $(u, v)$  for the STIRAP, where  $E_2 < E_1 < E_3$ .

where  $u = (u, v) \in \mathbb{R}^2$ . Let  $(\phi_n)_{n \geq 1}$  be a Hilbertian basis of  $\mathcal{H}$ , and assume that  $H(u, v)$  can be written in this basis as

$$H(u, v) = \begin{pmatrix} 0 & u & 0 & 0 & 0 & \cdots \\ u & \delta & v & 0 & 0 & \ddots \\ 0 & v & \omega & u & 0 & \ddots \\ 0 & 0 & u & \delta + \omega & v & \ddots \\ 0 & 0 & 0 & v & 2\omega & \ddots \\ \vdots & \ddots & \ddots & \ddots & \ddots & \ddots \end{pmatrix}, \quad (11)$$

where  $\delta, \omega > 0$ .

The Hamiltonian  $H(u, v)$  is self-adjoint with a purely discrete spectrum. Moreover, if  $uv \neq 0$ , then all eigenvalues of  $H(u, v)$  are non-degenerate (see [1, 4]).

Along the axis  $v = 0$ , one can show that the smallest value of  $|u|$  for which  $H(u, 0)$  has degenerate eigenvalues is  $u^* = \sqrt{\omega^2 - \delta^2}$ . This point is a conical intersection for  $H(u, v)$  between the levels  $\lambda_{2j}$  and  $\lambda_{2j+1}$  for every  $j \geq 1$ , at which Condition **(C)** is satisfied for similar reasons as those used in the proof of Proposition 6.1. We can deduce by the results of Section 2.2 that  $\chi_{2j, 2j+1}$  has a type **(N)** singularity at  $(\pm u^*, 0)$ , and by applying Theorem 5.1, that  $\chi_{2j-1, 2j}$  has a Darbouxian singularity at  $(\pm u^*, 0)$ .

Along the axis  $u = 0$ , we get that the smallest value of  $|v|$  for which  $H(0, v)$  has degenerate eigenvalues is  $v^* = \sqrt{\delta(2\omega - \delta)}$ . This point is a conical intersection for  $H(u, v)$  between the levels  $\lambda_{2j-1}$  and  $\lambda_{2j}$  for every  $j \geq 2$ . The smallest value of  $|v|$  for which 0 is a degenerate eigenvalue for  $H(0, v)$  is  $v_0^* = \sqrt{\delta\omega}$ , and it corresponds to a conical intersection between the levels  $\lambda_1$  and  $\lambda_2$ . The

latter points  $(0, \pm v^*)$  and  $(0, \pm v_0^*)$  are conical intersections for  $H(u, v)$  between the levels  $\lambda_{2j-1}$  and  $\lambda_{2j}$  for  $j \geq 1$  at which Condition **(C)** is satisfied for similar reasons as those used in the proof of Proposition 6.1. We can deduce by the results of Section 2.2 that  $\chi_{2j-1, 2j}$  has a type **(N)** singularity and, by applying Theorem 5.1, that  $\chi_{2j, 2j+1}$  has a Darbouxian singularity at those point.

## A Properties of two-level Hamiltonians, normal forms and proof of Proposition 4.4

### A.1 Generic families and equivalence of two-level Hamiltonians

What follows is directly taken from [5], and aims at presenting the admissible transformations considered in [5] for a two level quantum system with Hamiltonian  $H_f$ , for  $f \in C^\infty(\mathbb{R}^{2+l}, \mathbb{R}^2)$ .

Consider a smooth function  $f = (f_1, f_2) : \mathbb{R}^2 \times \mathbb{R}^l \rightarrow \mathbb{R}^2$  with  $l = 0$  or  $l = 1$ , and

$$H_f = \begin{pmatrix} f_1 & f_2 \\ f_2 & -f_1 \end{pmatrix}.$$

Denote by  $(e_1, \dots, e_{2+l})$  the canonical basis of  $\mathbb{R}^{2+l}$ . Given a vector  $\eta \in \mathbb{R}^{2+l}$  and a smooth function  $g : \mathbb{R}^{2+l} \rightarrow \mathbb{R}^q$ ,  $q \in \mathbb{N}$ , we write  $\partial_\eta g$  for the directional derivative of  $g$  in the direction  $\eta$  and  $\partial_i$  for  $\partial_{e_i}$ ,  $i = 1, \dots, 2+l$ . The coordinates  $(x_1, x_2)$  play the role of controls, and are denoted by  $(u, v)$ , while—in the case  $l = 1$ —the coordinate  $x_3$  is a parameter and is denoted by  $z$ . The space  $C^\infty(\mathbb{R}^{2+l}, \mathbb{R}^2)$  is endowed with the  $C^\infty$ -Whitney topology.

#### A.1.1 Genericity

We say that a property *is satisfied by a generic*  $f \in C^\infty(\mathbb{R}^{2+l}, \mathbb{R}^2)$  (or, equivalently, that it *holds generically with respect to*  $f$ ) if there exists an open and dense subset  $\mathcal{O}$  of the space  $C^\infty(\mathbb{R}^{2+l}, \mathbb{R}^2)$  such that the property holds for every  $f \in \mathcal{O}$ .

The main tool used for studying the genericity is Thom's transversality theorem, which ensures that a property is generic there exists a semi-algebraic set  $A$  of codimension at least  $3 + l$  in the jet space of the functions from  $\mathbb{R}^{2+l}$  to  $\mathbb{R}^2$  such that the property holds when the jet of  $f$  does not cross  $A$  (see, e.g., [14, 15]).

#### A.1.2 Equivalence of Hamiltonians

**Definition A.1.** We say that two elements  $f$  and  $\tilde{f}$  of  $C^\infty(\mathbb{R}^2, \mathbb{R}^2)$  (respectively,  $C^\infty(\mathbb{R}^3, \mathbb{R}^2)$ ) are time-equivalent at 0 if there exists a nowhere-vanishing function  $\xi \in C^\infty(\mathbb{R}^2, \mathbb{R})$  such that  $\tilde{f}(u, v) = \xi(u, v)f(u, v)$  (respectively,  $\tilde{f}(u, v, z) = \xi(u, v)f(u, v, z)$ ) in a neighborhood of 0.

**Definition A.2.** We say that two elements  $f$  and  $\tilde{f}$  of  $C^\infty(\mathbb{R}^3, \mathbb{R}^2)$  or  $C^\infty(\mathbb{R}^2, \mathbb{R}^2)$  are left-equivalent if there exists  $P \in O_2(\mathbb{R})$  independent of  $u, v, z$  such that  $H_f = PH_{\tilde{f}}P^{-1}$ .

**Definition A.3.** We say that two elements  $f$  and  $\tilde{f}$  of  $C^\infty(\mathbb{R}^2, \mathbb{R}^2)$  are right-equivalent at 0 if there exists a diffeomorphism  $\phi \in C^\infty(\mathbb{R}^2, \mathbb{R}^2)$  such that  $\phi(0) = 0$  and  $\tilde{f} = f \circ \phi$  in a neighborhood of 0.

**Definition A.4.** We say that two elements  $f$  and  $\tilde{f}$  of  $C^\infty(\mathbb{R}^3, \mathbb{R}^2)$  are right-equivalent at 0 if there exists a diffeomorphism  $\phi \in C^\infty(\mathbb{R}^3, \mathbb{R}^3)$  of the form  $\phi : (u, v, z) \mapsto (\phi_1(u, v), \phi_2(u, v), \phi_3(z))$ , where  $\phi_1, \phi_2 \in C^\infty(\mathbb{R}^2, \mathbb{R})$  and  $\phi_3 \in C^\infty(\mathbb{R}, \mathbb{R})$ , satisfying  $\phi(0) = 0$  and  $\tilde{f} = f \circ \phi$  in a neighborhood of 0.

By combination of the previous three definitions, we use the following notion of equivalence.

**Definition A.5.** We say that two elements  $f$  and  $\tilde{f}$  of  $C^\infty(\mathbb{R}^2, \mathbb{R}^2)$  are equivalent at 0 if there exists  $(\phi, \theta, \xi) \in C^\infty(\mathbb{R}^2, \mathbb{R}^2) \times \mathbb{S}^1 \times C^\infty(\mathbb{R}^2, \mathbb{R} \setminus \{0\})$  with  $\phi$  as in Definition A.4, and  $\zeta = \pm 1$  such that for every  $(u, v, z)$  in a neighborhood of 0,

$$\begin{cases} \tilde{f}_1(u, v) = \xi(u, v)(\cos(2\theta)f_1 \circ \phi(u, v) - \zeta \sin(2\theta)f_2 \circ \phi(u, v)), \\ \tilde{f}_2(u, v) = \xi(u, v)(\sin(2\theta)f_1 \circ \phi(u, v) + \zeta \cos(2\theta)f_2 \circ \phi(u, v)). \end{cases}$$

**Definition A.6.** We say that two elements  $f$  and  $\tilde{f}$  of  $C^\infty(\mathbb{R}^3, \mathbb{R}^2)$  are equivalent at 0 if there exists  $(\phi, \theta, \xi) \in C^\infty(\mathbb{R}^3, \mathbb{R}^3) \times \mathbb{S}^1 \times C^\infty(\mathbb{R}^2, \mathbb{R} \setminus \{0\})$  with  $\phi$  as in Definition A.4, and  $\zeta = \pm 1$  such that for every  $(u, v, z)$  in a neighborhood of 0,

$$\begin{cases} \tilde{f}_1(u, v, z) = \xi(u, v)(\cos(2\theta)f_1 \circ \phi(u, v, z) - \zeta \sin(2\theta)f_2 \circ \phi(u, v, z)), \\ \tilde{f}_2(u, v, z) = \xi(u, v)(\sin(2\theta)f_1 \circ \phi(u, v, z) + \zeta \cos(2\theta)f_2 \circ \phi(u, v, z)). \end{cases}$$

## A.2 Normal forms

With the notations of Section A.1, an eigenvalue intersection of  $H_f$  is a point in  $\mathbb{R}^2 \times \mathbb{R}^l$  where  $f$  vanishes.

### A.2.1 Conical intersection

An eigenvalue intersection  $(u, v)$  is conical if  $\mathcal{A}(f) := \det(\nabla f_1, \nabla f_2)$  is nonzero at  $(u, v)$ .

**Theorem A.7.** Assume that 0 is conical for  $f \in C^\infty(\mathbb{R}^2, \mathbb{R})$ . Then  $f$  is equivalent to  $Id_{\mathbb{R}^2}$ .

### A.2.2 Semi-conical intersection

An eigenvalue intersection  $(u, v)$  is semi-conical if  $\nabla f_1(\bar{u}, \bar{v})$  and  $\nabla f_2(\bar{u}, \bar{v})$  are collinear, are not both zero, and the directional derivative of  $\mathcal{A}(f)(\bar{u}, \bar{v})$  along  $\eta = (-\partial_2 f_j(\bar{u}, \bar{v}), \partial_1 f_j(\bar{u}, \bar{v}))$  is nonzero if  $j \in \{1, 2\}$  is such that  $\eta \neq 0$ . The direction spanned by  $\eta$  is the non-conical direction at  $(\bar{u}, \bar{v})$ .

**Theorem A.8** ([5]). Assume that 0 is semi-conical for  $f \in C^\infty(\mathbb{R}^2, \mathbb{R}^2)$ . Then  $f$  is equivalent to  $(u, v) \mapsto \begin{pmatrix} h(u)u \\ u + v^2 \end{pmatrix}$  where  $h : \mathbb{R} \rightarrow \mathbb{R}$  is a smooth function satisfying  $h(0) = 1$ .

The **algorithm** that is referred as **(A)** in the article [5, Section 2.3] to get the normal form consists in three steps:

- **STEP 1:** By a left-equivalence we transform  $f_1$  and  $f_2$  into two functions  $\tilde{f}_1$  and  $\tilde{f}_2$  such that  $\nabla \tilde{f}_1(0) = \nabla \tilde{f}_2(0) \neq 0$ .
- **STEP 2:** By a right-equivalence, we bring the non-conical direction to  $\text{span}(e_2)$ .
- **STEP 3:** By a further right-equivalence then a time-equivalence we transform  $f$  into the announced form.

Here we improve the results of [5] in order to be able to prove Proposition 4.4. Concatenating the three steps of Algorithm **(A)**, we are going to see that we can define a surjective mapping  $f \mapsto h_f$  from the set of functions in  $C^\infty(\mathbb{R}^2, \mathbb{R}^2)$  having a semi-conical intersection at 0 to the set of functions in  $C^\infty(\mathbb{R}, \mathbb{R})$  that are equal to 1 at 0, where for every  $f$ ,  $h_f$  corresponds to the function  $h$  obtained by the Algorithm **(A)**. Moreover, we can prove that

$$V_M = \{j^2(f)(0, 0) \in J^2(\mathbb{R}^2, \mathbb{R}^2) \mid 0 \text{ is a semi-conical intersection for } f, h'_f(0) = 0\}$$

is a closed Whitney stratified set of codimension 4.

In order to prove this statement, consider the coordinates  $(x_{jk} = \partial_j f_k(0))_{j,k \in \{1,2\}}$ ,  $(\tilde{x}_{jk} = \partial_j \tilde{f}_k(0))_{j,k \in \{1,2\}}$ ,  $(y_{jk}^l = \partial_{jk}^2 f_l(0))_{j,k,l \in \{1,2\}}$ , and  $(\tilde{y}_{jk}^l = \partial_{jk}^2 \tilde{f}_l(0))_{j,k,l \in \{1,2\}}$  in  $J^2(\mathbb{R}^2, \mathbb{R}^2)$ . The two first steps transform a function  $f \in C^\infty(\mathbb{R}^2, \mathbb{R}^2)$  into a function  $\tilde{f} \in C^\infty(\mathbb{R}^2, \mathbb{R}^2)$  such that

$$f(0) = 0, \partial_2 f(0) = 0, \partial_1 f_1(0) = \partial_1 f_2(0) \neq 0, \partial_2 \mathcal{A}(f)(0) \neq 0. \quad (\mathbf{SC})$$

**FIRST STEP:** For the first step of the Algorithm **(A)**, consider an arbitrary function  $f = (f_1, f_2) \in C^\infty(\mathbb{R}^2, \mathbb{R}^2)$  having a semi-conical intersection at 0. Without loss of generality, we can assume  $\nabla f_1(0) \neq 0$ , and define  $\alpha \in \mathbb{R}$  as the unique real number such that  $\nabla f_2(0) = \alpha \nabla f_1(0)$  (see [5, Definition 2.2]). Notice that the first order derivatives of  $f$  at 0 are uniquely determined by  $\nabla f_1(0)$  and  $\alpha$ , and that we have  $\tilde{x}_{12} = \tilde{x}_{11}$  and  $\tilde{x}_{22} = \tilde{x}_{21}$ .

One can show (see [2, Section 4.2 p. 94]) that the transformation achieved in this step is such that, for every  $(u, v)$ ,

$$\begin{pmatrix} \tilde{f}_1(u, v) \\ \tilde{f}_2(u, v) \end{pmatrix} = M(\alpha) \begin{pmatrix} f_1(u, v) \\ f_2(u, v) \end{pmatrix},$$

where

$$M(\alpha) = \frac{1}{\sqrt{2 + 2\alpha^2}} \begin{pmatrix} 1 + \alpha & \alpha - 1 \\ \alpha - 1 & 1 + \alpha \end{pmatrix}.$$

Hence the mapping

$$((x_{j1})_{j \in \{1,2\}}, \alpha) \mapsto ((\tilde{x}_{j1})_{j \in \{1,2\}})$$

is a submersion from  $(\mathbb{R}^2 \setminus \{(0,0)\}) \times \mathbb{R}$  to  $\mathbb{R}^2 \setminus \{(0,0)\}$ . It follows that

$$F : ((x_{j1})_{j \in \{1,2\}}, (y_{jk}^l)_{j,k,l \in \{1,2\}}, \alpha) \mapsto ((\tilde{x}_{j1})_{j \in \{1,2\}}, (\tilde{y}_{jk}^l)_{j,k,l \in \{1,2\}})$$

is a submersion from  $\mathbb{R}^9$  to  $\mathbb{R}^8$ .

**SECOND STEP:** For the second step of the Algorithm **(A)**, an arbitrary function  $f \in C^\infty(\mathbb{R}^2, \mathbb{R}^2)$  such that  $\nabla f_1(0) = \nabla f_2(0)$  is transformed by right-equivalence into  $\hat{f}(u, v) = f(\partial_1 f_1(0)u - \partial_2 f_1(0)v, -\partial_2 f_1(0)u + \partial_1 f_1(0)v)$ , so that we have  $\partial_1 \hat{f}_1(0) = \partial_1 \hat{f}_2(0)$ , and  $\partial_2 \hat{f}_1(0) = \partial_2 \hat{f}_2(0) = 0$ . By direct computations, we can show that the mapping

$$\hat{F} : ((x_{j1})_{j \in \{1,2\}}, (y_{jk}^l)_{j,k,l \in \{1,2\}}) \mapsto (\hat{x}_{11}, (\hat{y}_{jk}^l)_{j,k,l \in \{1,2\}})$$

is a submersion from  $\mathbb{R}^8$  to  $\mathbb{R}^7$ .

By composition of submersions, we obtain that  $\hat{F} \circ F$  is a submersion from  $\mathbb{R}^9$  to  $\mathbb{R}^7$ .

**THIRD STEP:** Concerning the third step of Algorithm **(A)**, we have the following result, whose proof can be found in [2, Lemma 4.2.29], and is obtained by adapting the computations of the proof of [5, Proposition 10].

**Lemma A.9.** *For a function  $f \in C^\infty(\mathbb{R}^2, \mathbb{R}^2)$  satisfying Condition **(SC)**, consider the function  $(u, v) \mapsto \begin{pmatrix} uh(u) \\ u + v^2 \end{pmatrix}$  obtained from  $f$  by the third step of Algorithm **(A)**, where  $h \in C^\infty(\mathbb{R}, \mathbb{R})$  is such that  $h(0) = 1$ . Then we have  $h'(0) = 0$  if and only if*

$$(\partial_{11} f_2(0,0) \partial_1 f_1(0,0) - \partial_1 f_2(0,0) \partial_{11} f_1(0,0)) \partial_2 \mathcal{A}(f)(0,0) = (\partial_1 \mathcal{A}(f)(0,0))^2. \quad (12)$$

Notice that Equality (12) is clearly independent from Condition (SC). Using Lemma A.9 and the fact that  $\hat{F} \circ F$  is a submersion from  $\mathbb{R}^9$  to  $\mathbb{R}^7$ , we can conclude that

$$V_M = \{j^2(f)(0, 0) \in J^2(\mathbb{R}^2, \mathbb{R}^2) \mid 0 \text{ is a semi-conical intersection for } f, h'_f(0) = 0\}$$

is a closed Whitney stratified set of codimension 4.

### A.3 Proof of Proposition 4.4

Consider now the set  $V_S = \{j^2(F)(0, 0, 0) \in J^2(\mathbb{R}^3, \mathbb{R}^2) \mid j^2(F(\cdot, \cdot, 0))(0, 0) \in V_M\}$  where  $j^2(F(\cdot, \cdot, 0))$  is the 2-jet of  $f(\cdot, \cdot) = F(\cdot, \cdot, 0)$  related to the variables  $u$  and  $v$ . By Thom's transversality theorem (see, e.g., [14]) used in combination with [15, §1.3.2], we can deduce that

$$\tilde{O} = \{F \in C^\infty(\mathbb{R}^3, \mathbb{R}^2), j^2F(\mathbb{R}^3) \cap V_S = \emptyset\}$$

is an open and dense subset of  $C^\infty(\mathbb{R}^3, \mathbb{R}^2)$ . We can deduce Proposition 4.4.

## B Useful results about line fields

Here we recall some results about line fields taken from [7] and we prove the theorems B.8 and B.9 which allow to prove Theorem 5.1.

**Definition B.1.** *Let  $(M, g)$  be a 2-dimensional Riemannian manifold. A line field on  $M$  is a section of  $PT(M \setminus K)$ , where  $K$  is a closed subset of  $M$ .*

**Definition B.2.** *Let  $(M, g)$  be a 2-dimensional Riemannian manifold. A proto-line-field is a pair  $(X, Y)$  of vector fields on  $M$ . Denote by  $z_X$  and  $z_Y$  the sets of zeros of  $X$  and  $Y$ . The line field associated with  $(X, Y)$ , denoted by  $B_g(X, Y)$ , is the section of  $PT(M \setminus (z_X \cup z_Y))$  defined at a point  $p \in M \setminus (z_X \cup z_Y)$  as the line  $B_g(X(p), Y(p))$  of  $T_pM$  bisecting  $(X(p), Y(p))$  for the metric  $g(p)$ .*

**Proposition B.3.** *Let  $(M, g)$  be a 2-dimensional Riemannian manifold,  $K$  be a closed subset of  $M$  and  $L$  be a section of  $PT(M \setminus K)$ . There exist two vector fields  $X$  and  $Y$  such that  $L = B_g(X, Y)$ .*

With this definition, the Whitney topology on pairs of vector fields on  $M$  defines a topology on line fields on  $M$ , the zeros of  $X$  and  $Y$  become singularities of the associated line-field.

**Definition B.4.** *A one-dimensional connected immersed submanifold  $N$  of  $M \setminus (z_X \cup z_Y)$  is said to be an integral manifold of the proto-line-field  $(X, Y)$  if for any point  $p$  of  $N$ , the tangent line to  $N$  at  $p$  is given by  $B_g(X, Y)$ .*

We say that a proto-line-field  $L$  has a *Darbouxian singularity* if its integral manifolds are locally homeomorphic to those of the proto-line-fields defined by  $(X_L, Y_L)$ ,  $(X_M, Y_M)$  and  $(X_S, Y_S)$  defined as follows:

- The *Lemon proto-line-field* (see Figure 23) is the pair of vector fields on  $(\mathbb{R}^2, Eucl)$  defined by

$$X_L(x, y) = \begin{pmatrix} x + y \\ y - x \end{pmatrix}, \quad Y_L(x, y) = \begin{pmatrix} 1 \\ 1 \end{pmatrix}.$$

- The *Monstar proto-line-field* (see Figure 24) is the pair of vector fields on  $(\mathbb{R}^2, Eucl)$  defined by

$$X_M(x, y) = \begin{pmatrix} x \\ 3y \end{pmatrix}, \quad Y_M(x, y) = \begin{pmatrix} 1 \\ 0 \end{pmatrix}.$$

- The *Star proto-line-field* (see Figure 25) is the pair of vector fields on  $(\mathbb{R}^2, Eucl)$  defined by

$$X_S(x, y) = \begin{pmatrix} x \\ -y \end{pmatrix}, \quad Y_S(x, y) = \begin{pmatrix} 1 \\ 0 \end{pmatrix}.$$

Darbouxian singularities have an index equal to  $\pm\frac{1}{2}$ .

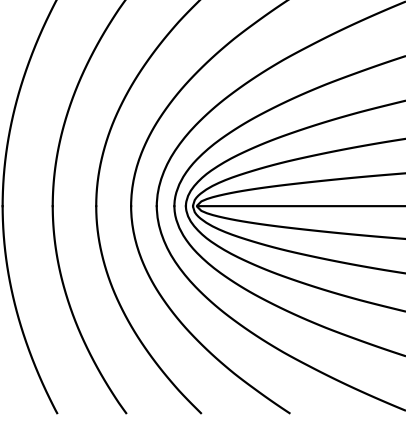


Figure 23: The Lemon singularity, of index  $\frac{1}{2}$ .

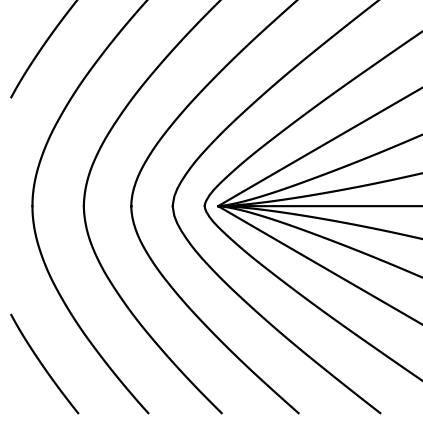


Figure 24: The Monstar singularity, of index  $\frac{1}{2}$ .

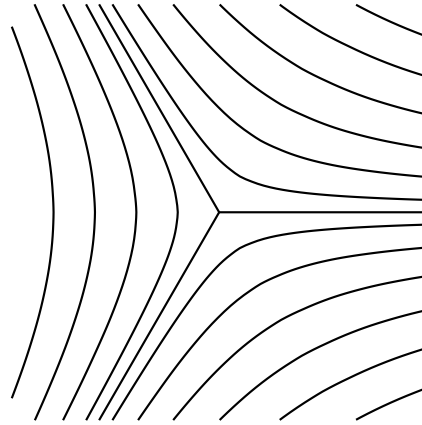


Figure 25: The Star singularity, of index  $-\frac{1}{2}$ .

**Definition B.5.** Let  $(X, Y)$  be a proto-line field on  $(M, g)$ , and  $(X', Y')$  be a proto-line-field on  $(M', g')$ . Fix  $p \in M$  and  $p' \in M'$ . Then  $(X, Y)$  and  $(X', Y')$  are said to be topologically equivalent at  $p$  and  $p'$  if there exist two neighborhoods  $V_p$  and  $W_{p'}$  of  $p$  and  $p'$  respectively and a homeomorphism  $h : V_p \rightarrow W_{p'}$ , with  $h(p) = p'$ , which takes the integral manifolds of  $(X, Y)$  onto those of  $(X', Y')$ .

**Definition B.6.** We say that a proto-line-field  $(X, Y)$  has a non-degenerate singularity (respectively, a hyperbolic singularity) at a point  $p \in M$  if one of the two vector fields has a non-degenerate singularity (respectively, a hyperbolic singularity) and the other is non-vanishing at  $p$ .

**Theorem B.7** (Hyperbolic singularities of line fields). Let  $(M, g)$  be a two-dimensional Riemannian manifold. Hyperbolic singularities of proto line fields on  $M$  are Darbouxian.

We prove here two new technical results about line fields that are used in the proof of Theorem 5.1.

**Proposition B.8** (Non-degenerate singularities of line fields). *Let  $(M, g)$  be a two-dimensional Riemannian manifold. Non-degenerate singularities of proto-line-fields on  $M$  are Darbouxian. Moreover, consider a proto line field  $(X, Y)$  on  $M$  such that  $\bar{p}$  is a non-degenerate singularity of  $(X, Y)$ . Then there exists two sequences  $(X_n)_{n \in \mathbb{N}}$  and  $(Y_n)_{n \in \mathbb{N}}$  of smooth vector fields on  $M$  converging respectively to  $X$  and  $Y$  for the  $C^\infty$ -Whitney topology, such that for every  $n \in \mathbb{N}$ ,  $\bar{p}$  is an hyperbolic singularity of  $(X_n, Y_n)$  and  $B_g(X(p), Y(p)) = B_g(X_n(p), Y_n(p))$  for  $p$  in a punctured neighborhood of  $\bar{p}$ .*

*Proof.* Consider a proto line field  $(X, Y)$  such that  $X$  has a non-degenerate zero at  $\bar{p} \in M$  and  $Y(\bar{p}) \neq 0$ . If  $\bar{p}$  is hyperbolic, then Theorem B.7 proves the result.

Assume now that  $X$  is non-degenerate and not hyperbolic at  $\bar{p}$ . Define  $\tilde{X}$  and  $\tilde{Y}$  as the smooth vector fields which are the image of respectively,  $X$  and  $Y$  by the rotation of angle  $\frac{\pi}{2}$  for the metric  $g$ . This construction is always possible, at least locally around  $\bar{p}$ . By using local charts, one can easily show that  $\tilde{X}$  is hyperbolic at  $\bar{p}$ . Define a neighborhood  $V$  of  $\bar{p}$  such that  $\tilde{X}$  and  $\tilde{Y}$  are well defined on  $V$  and  $\bar{p}$  is the only zero of  $X$  in  $V$ ,  $Y$  is non-zero on  $V$ , and set  $W = V \setminus \{\bar{p}\}$ . We can notice that for every  $p \in W$ ,  $\frac{\tilde{X}(p)}{\|\tilde{X}(p)\|} - \frac{\tilde{Y}(p)}{\|\tilde{Y}(p)\|}$  is colinear to  $B_g(X(p), Y(p))$ , hence we can deduce the equality  $B_g(X(p), Y(p)) = B_g(\tilde{X}(p), -\tilde{Y}(p))$ . By construction,  $\bar{p}$  is hyperbolic for  $(\tilde{X}, \tilde{Y})$ , hence Theorem B.7 proves that  $\bar{p}$  is Darbouxian. The first claim is proved. In order to prove the second claim, define, for  $p$  in  $W$  and  $\epsilon > 0$ ,  $X_\epsilon(p) = X(p) + \epsilon\tilde{X}(p)$  and  $Y_\epsilon(p) = Y(p) - \epsilon\tilde{Y}(p)$ . By construction of  $\tilde{X}$  and  $\tilde{Y}$ , we have, for every  $p$  in  $W$ ,  $\|X_\epsilon(p)\| = \sqrt{1 + \epsilon^2}\|X(p)\|$  and  $\|Y_\epsilon(p)\| = \sqrt{1 + \epsilon^2}\|Y(p)\|$ . It follows that, for  $p$  in  $W$ ,  $\frac{X_\epsilon(p)}{\|X_\epsilon(p)\|} + \frac{Y_\epsilon(p)}{\|Y_\epsilon(p)\|} = \frac{1}{\sqrt{1 + \epsilon^2}} \left( \left( \frac{X(p)}{\|X(p)\|} + \frac{Y(p)}{\|Y(p)\|} \right) + \epsilon \left( \frac{\tilde{X}(p)}{\|\tilde{X}(p)\|} - \frac{\tilde{Y}(p)}{\|\tilde{Y}(p)\|} \right) \right)$ . Noticing that for  $p$  in  $W$ ,  $\frac{\tilde{X}(p)}{\|\tilde{X}(p)\|} - \frac{\tilde{Y}(p)}{\|\tilde{Y}(p)\|}$  and  $\frac{X(p)}{\|X(p)\|} + \frac{Y(p)}{\|Y(p)\|}$  are colinear to  $B_g(X(p), Y(p))$ , we can deduce that  $\frac{X_\epsilon(p)}{\|X_\epsilon(p)\|} + \frac{Y_\epsilon(p)}{\|Y_\epsilon(p)\|}$  is colinear to  $B_g(X(p), Y(p))$ . Hence  $B_g(X(p), Y(p)) = B_g(X_\epsilon(p), Y_\epsilon(p))$ , for every  $p \in W$ . The hyperbolicity of  $\tilde{X}$  at  $\bar{p}$  implies that  $X_\epsilon$  is hyperbolic at  $\bar{p}$ . Moreover, for  $\epsilon > 0$ , we have  $Y_\epsilon(\bar{p}) \neq 0$ . For such  $\epsilon$ ,  $\bar{p}$  is a hyperbolic singularity for the proto-line-field  $(X_\epsilon, Y_\epsilon)$ . Setting for  $n \geq 1$ ,  $\epsilon_n = \frac{1}{n}$  and  $X_n = X_{\epsilon_n}$ ,  $Y_n = Y_{\epsilon_n}$ , we have clearly that  $(X_n)_n$  and  $(Y_n)_n$  converge respectively to  $X$  and  $Y$  for the  $C^\infty$ -Whitney topology. The result is proved.  $\square$

**Theorem B.9.** *Consider a two dimensional Riemannian manifold  $(M, g)$ . Let  $L$  be a line field on  $M$  and  $A$  a smooth section of  $GL(TM) = \cup_{p \in M} GL(T_p M)$ . Denote by  $K \subset M$  the closed set of singular points of  $L$ . Let  $\tilde{L}$  be the line field defined on  $M$  by  $\tilde{L}(p) = A(p)(L(p))$  (where the equality is defined as the equality of the associated directions in  $T_p M$ ) for every  $p \in M \setminus K$ . Let  $\bar{p} \in K$ . Consider two vector fields  $X$  and  $Y$  on  $M$  such that, for every  $p \in M \setminus K$ ,  $L(p) = B_g(X(p), Y(p))$ , and satisfying the conditions  $X(\bar{p}) = 0$ ,  $DX(\bar{p})$  is non-degenerate, and  $Y(\bar{p}) \neq 0$ . Then there exists a metric  $\tilde{g}$  on  $M$  such that, for every  $p \in M \setminus K$ ,  $\tilde{L}(p) = B_{\tilde{g}}(A(p)X(p), A(p)Y(p))$ . Moreover  $p$  is non-degenerate for  $(AX, AY)$  if and only if  $p$  is non-degenerate for  $(X, Y)$ .*

*Proof.* Define the metric  $\tilde{g}$  by  $\tilde{g}(p)(x, y) = g(p)(A^{-1}(p)x, A^{-1}(p)y)$  for every  $p \in M$  and  $(x, y) \in T_p M \times T_p M$ . Then we get easily that, for every  $p \in M \setminus K$ ,  $\tilde{L}(p) = B_{\tilde{g}}(A(p)X(p), A(p)Y(p))$ . Let  $\bar{p} \in K$ . Using the conditions  $A(\bar{p}) \in GL(T_{\bar{p}} M)$ , we have  $A(\bar{p})Y(\bar{p}) \neq 0$ ,  $A(\bar{p})X(\bar{p}) = 0$ , and that  $D(AX)(\bar{p})$  is non-degenerate. The theorem is proved.  $\square$

## Acknowledgments

The author is grateful to Mario Sigalotti and Ugo Boscain for their suggestions and for very helpful discussions.

This work was supported in part by the ANR project Maximic (ANR-17-CE40-0024-01), ANR project Quaco ANR-17-CE40-0007-01 and the ANR project ICycle (ANR-16-CE33-0016-01).

## References

- [1] R. Adami and U. Boscain. Controllability of the schrödinger equation via intersection of eigenvalues. In *Proceedings of the 44th IEEE Conference on Decision and Control*, pages 1080–1085, Dec 2005.
- [2] N. Augier. *Adiabatic control of quantum systems*. PhD thesis, Université Paris Saclay (COMUE), Sept. 2019. <https://tel.archives-ouvertes.fr/tel-02434725/document>.
- [3] N. Augier, U. Boscain, and M. Sigalotti. Effective adiabatic control of a decoupled hamiltonian obtained by rotating wave approximation. *Preprint HAL*. <https://hal.inria.fr/hal-02562363v2/document>.
- [4] N. Augier, U. Boscain, and M. Sigalotti. Adiabatic Ensemble Control of a Continuum of Quantum Systems. *SIAM J. Control Optim.*, 56(6):4045–4068, 2018.
- [5] N. Augier, U. Boscain, and M. Sigalotti. Semi-conical eigenvalue intersections and the ensemble controllability problem for quantum systems. *Math. Control Relat. Fields*, 2020.
- [6] A. M. Bloch, R. W. Brockett, and C. Rangan. Finite controllability of infinite-dimensional quantum systems. *IEEE Trans. Automat. Control*, 55(8):1797–1805, 2010.
- [7] U. Boscain, L. Sacchelli, and M. Sigalotti. Generic singularities of line fields on 2D manifolds. *Differential Geom. Appl.*, 49:326–350, 2016.
- [8] U. V. Boscain, F. Chittaro, P. Mason, and M. Sigalotti. Adiabatic control of the Schrödinger equation via conical intersections of the eigenvalues. *IEEE Trans. Automat. Control*, 57(8):1970–1983, 2012.
- [9] S. Chelkowski, A. D. Bandrauk, and P. B. Corkum. Efficient molecular dissociation by a chirped ultrashort infrared laser pulse. *Phys. Rev. Lett.*, 65:2355–2358, Nov 1990.
- [10] F. C. Chittaro and P. Mason. Approximate controllability via adiabatic techniques for the three-inputs controlled Schrödinger equation. *SIAM J. Control Optim.*, 55(6):4202–4226, 2017.
- [11] R. Dann and R. Kosloff. Inertial theorem: Overcoming the quantum adiabatic limit. *Phys. Rev. Research*, 3:013064, Jan 2021.
- [12] F. Dumortier, J. Llibre, and J. Artés. Qualitative theory of planar differential systems. *Qualitative Theory of Planar Differential Systems*, 06 2007.
- [13] S. J. Glaser, U. Boscain, T. Calarco, C. P. Koch, W. Köckenberger, R. Kosloff, I. Kuprov, B. Luy, S. Schirmer, T. Schulte-Herbrüggen, D. Sugny, and F. K. Wilhelm. Training schrödinger’s cat: quantum optimal control. *The European Physical Journal D*, 69(12):279, 2015.
- [14] M. Golubitsky and V. Guillemin. *Stable mappings and their singularities*. Springer-Verlag, New York-Heidelberg, 1973. Graduate Texts in Mathematics, Vol. 14.
- [15] M. Goresky and R. MacPherson. *Stratified Morse Theory*. Springer Berlin Heidelberg, Berlin, Heidelberg, 1988.



- [16] S. Guérin. Complete dissociation by chirped laser pulses designed by adiabatic floquet analysis. *Phys. Rev. A*, 56:1458–1462, Aug 1997.
- [17] S. Guérin, S. Thomas, and H. R. Jauslin. Optimization of population transfer by adiabatic passage. *Phys. Rev. A*, 65:023409, Jan 2002.
- [18] G. A. Hagedorn. Classification and normal forms for quantum mechanical eigenvalue crossings. *Astérisque*, (210):7, 115–134, 1992. Méthodes semi-classiques, Vol. 2 (Nantes, 1991).
- [19] G. A. Hagedorn. Classification and normal forms for avoided crossings of quantum-mechanical energy levels. *Journal of Physics A: Mathematical and General*, 31(1):369–383, jan 1998.
- [20] G. A. Hagedorn and A. Joye. Molecular propagation through small avoided crossings of electron energy levels. *Rev. Math. Phys.*, 11(1):41–101, 1999.
- [21] F. Laudenbach. Homologie de morse dans la perspective de l’homologie de floer. *Mini-cours dans le cadre de la rencontre GIRAGA XIII, Yaoundé*, 2010.
- [22] C. K. Law and J. H. Eberly. Arbitrary control of a quantum electromagnetic field. *Phys. Rev. Lett.*, 76:1055–1058, Feb 1996.
- [23] H. L. Mortensen, J. J. W. H. Sørensen, K. Mølmer, and J. F. Sherson. Fast state transfer in a lambda-system: a shortcut-to-adiabaticity approach to robust and resource optimized control. *New Journal of Physics*, 20(2):025009, feb 2018.
- [24] R. Robin, N. Augier, U. Boscain, and M. Sigalotti. Ensemble qubit controllability with a single control via adiabatic and rotating wave approximations. *Preprint HAL*. <https://hal.archives-ouvertes.fr/hal-02504532v2/document>.
- [25] B. W. Shore. *The Theory of Coherent Atomic Excitation, Volume 1, Simple Atoms and Fields*. July 1990.
- [26] S. Teufel. *Adiabatic perturbation theory in quantum dynamics*, volume 1821 of *Lecture Notes in Mathematics*. Springer-Verlag, Berlin, 2003.
- [27] N. V. Vitanov. High-fidelity multistate stimulated raman adiabatic passage assisted by shortcut fields. *Physical Review A*, 102(2):023515, 2020.
- [28] N. V. Vitanov, T. Halfmann, B. W. Shore, and K. Bergmann. Laser-induced population transfer by adiabatic passage techniques. *Annual Review of Physical Chemistry*, 52(1):763–809, 2001.
- [29] H. Yuan and S. Lloyd. Controllability of the coupled spin- $\frac{1}{2}$  harmonic oscillator system. *Phys. Rev. A*, 75:052331, May 2007.